Transport and sorption phenomena in concrete and other porous media

Johannesson, Björn

2000

LUND UNIVERSITY
LUND INSTITUTE OF TECHNOLOGY
Division of Building Materials

TRANSPORT AND SORPTION PHENOMENA IN CONCRETE AND OTHER POROUS MEDIA

Björn Johannesson

Report TVBM - 1019

Doctoral Thesis

Lund 2000

LUND UNIVERSITY
LUND INSTITUTE OF TECHNOLOGY
Division of Building Materials

TRANSPORT AND SORPTION PHENOMENA IN CONCRETE AND OTHER POROUS MEDIA

Björn Johannesson

Report TVBM - 1019 Doctoral Thesis

Lund 2000

ISRN: LUTVDG/TVBM–00/1019–SE(1-227)
ISSN: 0348-7911 TVBM
ISBN: 91-628-4351-6

Lund Institute of Technology
Division of Building Materials
Box 118
SE-221 00 Lund, Sweden

Telephone: +46-46-2224052
Telefax: +46-46-2224427
WWW: http://www.ldc.lu.se/lthbml

Preface

This work has been carried out at the Division of Building Materials at the Lund Institute of Technology and has been financed by the Swedish Foundation for Concrete Research (Stiftelsen Svensk Betongforskning) and the Swedish Council for Building Research (Byggforskningsrådet, BFR) which are gratefully acknowledged. The research project was initiated by my supervisor, Professor Göran Fagerlund, whom I wish to thank for his support.

I would like to thank dr. Manouchehr Hassanzadeh and the rest of the staff at the Division of Building Materials for their help and support during the process.

QUOTATIONS

From pp. 92-93 of *Six Lectures on Modern Natural Philosophy:* VI. Method and Taste in Natural Philosophy. Berlin: Springer-Verlag, 1966.

> The hard facts of classical mechanics taught to undergraduates today are, in their present forms, creations of James and John Bernoulli, Euler, Lagrange, and Cauchy, men who never touched a piece of apparatus; their only researches that have been discarded and forgotten are those where they tried to fit theory to experimental data. They did not disregard experiment; the parts of their work that are immortal lie in domains where experience, experimental or more common, was at hand, already partly understood through various special theories, and they abstracted and organized it and them. To warn scientists today not to disregard experiment is like preaching against atheism in church or communism among congressmen. It is cheap rabble-rousing. The danger is all the other way. Such a mass of experimental data on everything pours out of organized research that the young theorist needs some insulation against its disrupting, disorganizing effect. Poincaré said, "The science must order; science is made out of facts as a house is made out of stones, but an accumulation of facts is no more science than a heap of stones, a house."
>
> *Clifford Truesdell*

From pp. 35 of *Six Lectures on Modern Natural Philosophy:* III. Thermodynamics of visco-elasticity. Berlin: Springer-Verlag, 1966.

> There is nothing that can be said by mathematical symbols and relations which cannot also be said by words. The converse, however, is false. Much that can be and is said by words cannot successfully be put into equations, because it is nonsense.
>
> *Clifford Truesdell*

Contents

TRANSPORT AND SORPTION PHENOMENA IN CONCRETE AND OTHER POROUS MEDIA

1 Organization of the thesis

This thesis consists of:

- An introductory background.
- Six reports divided into three groups or parts: Part I, *Chloride ingress in concrete* (3 reports), Part II, *Moisture transport* (1 report) and Part III, *Moisture fixation* (2 reports).
- Eight papers, published or submitted for publication.

The *introductory background* give a rather condensed account of the contents of the different reports and papers. Besides, it gives a short review of the characteristics of concrete and of different destruction types where transport phenomena are of interest. It also give information on how chloride profiles, moisture transport coefficients and moisture fixation are measured.

The *reports* give a more comprehensive theoretical description of different transport phenomena and of fixation of moisture. Some *papers* are based on the reports. Others papers contain additional theory and experimental data besides what is found in the reports.

2 Summary of the thesis

2.1 General remarks on transport phenomena and durability

Degradation processes such as frost attack and steel corrosion in cement-based porous materials cause society considerable costs yearly. Therefore it is interesting to find a methodology to predict the performance of a structure in advance. Such a methodology can be used in order to avoid expensive repair and also as a guideline when choosing materials and when designing constructions.

Many of the durability problems of concrete structure are directly or indirectly associated with the condition of the pore solution. This thesis is addressed towards the determination of the main properties affecting the condition of the pore solution in concrete, e.g. the effect on concrete quality of chloride penetration and leaching of hydroxide ions, the effect of capillary suction on ion diffusion in a pore system and the effect of dielectrics on diffusion of different types of dissolved positive and negative ions.

Degradation mechanisms of concrete structures being directly related to the physical and chemical conditions in the pore solution are, for example: *(i)* reinforcement corrosion, *(ii)* salt-frost scaling, *(iii)* carbonation and *(iv)* sulfate attack.

Today, constructions are indeed designed using powerful computer tools where deformations and stresses may be calculated with acceptable accuracy for both static loads and more complex dynamic load cases. A wide range of experimentally verified complex constitutive behaviors in terms of stresses and strains for different materials are implemented in such computer programs. These programs are used by civil engineers every day. It is the author's opinion that the reason such material models are gaining great popularity is due to the use of a stringent theory in which the material assumptions have a clear and physical meaning. The usefulness of such material models in designing structures is obvious. In fact, modern models dealing with, for example, material and geometrical non-linearities, elasticity and plasticity are based on over a hundred years of research.

The service life of a structure is not, however, determined solely by its resistance to maximum possible static and dynamic load cases in its initial virgin state. Instead, degradation of the bulk material and the material surfaces caused by environmentally induced effects such as reinforcement cor-

rosion, deicing salt scaling, chemical attack, etc., determine the service life. This means that the change of the material properties with time must be searched for in order to evaluate the expected deterioration and service life of a structure. By studying the mechanism of, for example, reinforcement corrosion and freezing and thawing of porous materials, one might eventually find physically relevant material parameters describing the degradation phenomena of interest. If these mechanisms could be understood and hence modeled, the change of the mechanical properties with time may be predicted. Besides, in order to make this prediction, the external environmental properties and their variations must be known.

Processes such as carbonation and chloride penetration causing reinforcement corrosion, development of cracks due to freezing and thawing of pore water, leaching of hydroxide ions, flow of vapor and liquid water, and development of global crack patterns due to mechanical loadings and creep are all phenomena of great interest in the field of durability of cementitious materials. In fact, many of the separate deterioration processes will accelerate or decelerate down each other when they act simultaneously. By 'durability' of structures is mainly meant service life with regard to such properties as determine the structural stability, i.e. strength, reinforcement corrosion, stiffness, etc. Hence, aesthetic damage, wear etc. are not normally considered and definitely not calculated theoretically or designed for.

As the problem of estimating the durability of structures is complex, a physically stringent model describing degradation phenomena is necessarily extensive. Hence, the governing equation system reflecting such behaviors ought to be complex too, even if the problem is simplified as much as tolerable.

Since important properties such as bearing capacity and maximum allowable deflections may be introduced as threshold values indicating the condition of a considered structure, it seems natural to use the concept of stress and deformation for estimating the service life of inorganic material structures with regard to structural stability. However, the determination of the stress and deformation state is very much a question of the presence and variation of the environmental conditions in terms of, for example, temperature, moisture and deleterious substances such as chloride ions, because these factors determine the 'inner climate' in the structure and thus the degradation rate and extent.

In this thesis only a small part of the durability problem is treated; for example, very little attention has been addressed to the description of the

stress strain behavior of concrete induced by the environment, such as cracks induced by chloride-induced reinforcement corrosion. Thus, the corrosion process is not considered, only the chloride inflow until a certain threshold concentration has been reached at the reinforcement bar. The effects of, for example, the reinforcement corrosion on the structural stability or other destruction phenomena such as freeze-thaw attack are not considered at all in the thesis.

The proposed material models in this thesis, describing diffusion of different types of ions in pore solution of cement-based materials, will without doubt be revised in the future. The use of physically stringent assumptions to describe such phenomena is, however, believed to be a fruitful way of developing significant experimental setups; hence realistic simulations in the field of durability may be performed. The present work is a step in this direction.

2.2 Summary of theories and results

The *Introductory background*, section 3, describes the important parameters; chemical composition of hardened cement, moisture and ion transport models, and common techniques for measuring and evaluating the moisture condition and ion diffusion properties.

The material concrete is described in section 3.1. The hydration of different compounds in cement and pozzolans is described. The hydration products formed, from cement and pozzolans reacting with water is one of the main factors determining the durability of concrete. Admixtures, of different types, are almost always used in modern concrete technology. The effects of these compounds on fresh and well-hydrated concrete are, therefore, also discussed.

In section 3.2 some of the most important degradation mechanisms of reinforced concrete structure are listed. Nearly all of these mechanisms are directly related to the composition of the pore solution, in terms of different types of dissolved ions, and of the solid hydration products of the cement and pozzolans in the concrete. The factor determining the change of the composition in the solid hydration products and in the pore solution is the external outer climate, e.g. presence of chloride ion solutions, low temperatures, sulfates, etc.

Mechanisms governing the diffusion of different types of ions are discussed in section 3.3.1. Most of the proposed mechanisms are incorporated

in a model of multicomponent ion diffusion in the pore solution of concrete described in section 3.3.2. Different parts of this problem are also treated in reports I:1-3 and papers 1-3.

In section 3.3.3 the most common ways of measuring chloride ion diffusion characteristics in the pore solution of concrete are discussed. The hypothesis on which the evaluation of these measurements is based is carefully described. The methods are general in the sense that other ion types than chlorides can be investigated with respect to penetration into concrete.

Section 3.5.1 describes different techniques for measuring the equilibrium moisture content in a material at different relative humidities in the surrounding air. This property, i.e. the sorption isotherm, is very important for ion diffusion when the moisture content is lower than at saturation. A newly developed method measuring sorption isotherms is presented in this section. This new method can also be used to predict the heat of condensation of different adsorbed layers on 'bare' material surfaces.

Different techniques for measuring moisture profiles for samples being exposed to drying or wetting are presented in section 3.4.4. Measured moisture profiles are often used to check the performance of moisture transport models. The moisture flow characteristics in concrete during different exposure conditions will heavily affect the different types of ions present in the pore solution. Methods for incorporating the moisture content and flow properties into models dealing with ion diffusion are discussed in section 3.3.2 of this introduction, and in papers 2 and 3.

Section 3.4.1 deals with a method for calculating the water diffusivity, as used in Fick's second law, as a function of water content from steady state measurements. Two different measurement methods can be adopted when evaluating this function: either the steady state moisture profile is measured for a give exposure condition, or the steady state flow using the cup-method. The method assumes that no transient sorption takes place, i.e. the moisture content is always assumed to be in equilibrium with the relative humidity given from the sorption isotherm. The results are, further, restricted to either wetting or drying since no special attention is paid to hysteresis effects in the sorption behavior. A model suitable for incorporating hysteresis and non-isothermal effects is presented in paper 8. This model allows for transient sorption characteristics. The calculated water diffusivity as a function of water content, using the approach outlined in section 3.4.1, is included as an important material parameter in the ion diffusion model described in section 3.3.2.

A less general method of calculating the water diffusivity as a function of water content than the one described in section 3.4.1, is discussed in section 3.4.2. This method is restricted in the sense that the mass gain during capillary suction in a one-dimensional, semi-infinite, test must be related to the exposure time with a square root dependence. In fact, many different materials fulfill this condition with acceptable accuracy. The experiments consist of a series of capillary suction experiments for different initial water contents in sample. From the measured mass gain, as a function of exposure time, for these experiments the water diffusivity as a function of water content can be calculated. The theoretical background making this calculation possible, for the given test conditions and theoretical restrictions, is described. The main benefit of the approach is that it is simple and experimentally inexpensive; further, the water diffusivity as a function of water content is calculated from the experimental results in an explicit manner. The capillary suction behavior is treated with a completely different approach in report II:1. This method is established from considering the momentum balance equation and mass balance equation together with an assumption for the stress tensor of the capillary water. Such an alternative model is supposed to give adequate information about the underlying mechanism of capillary suction not available when using the traditional moisture transport models, e.g. Fick's second law.

In section 3.4.3 it is argued that a more detailed model than those described in sections 3.4.1 and 3.4.2 concerning moisture transport models must be established when effects such as hysteresis in sorption and temperature changes are to be included. The proposed model is based on having a separate description of the water vapor and liquid water in the pore system of material. In paper 8 such a model is compared with measurements on moisture profiles and kinetics of sorption on cement mortar.

The mass transport models described in reports I:1-3, report II:1, paper 2 and paper 8 needs information about material properties, such as porosity, specific surface area and pore size distribution. The porosity and the degree of water saturation in a pore system very much determine the diffusion resistance of ions dissolved in a pore solution. The specific surface area is a key factor for determining some of the properties related to the reactivity between ions in a pore solution and the solid hydration products. The hypotheses used as a basis when predicting pore size distribution and specific surface area from sorption measurements are described in section 3.5.2. These concepts are used in reports III:1-2 and paper 7. In these reports an

important part is devoted to determining the heat of condensation of different adsorbed layers on 'bare' material surfaces, which can be obtained from measurements on sorption using a microcalorimetric approach together with assumptions introduced in the BET theory. The reason for examining this property, which is not directly related to mass transport of water and dissolved ions in the pore system of cement based materials, is that the basic assumptions in the BET theory can be examined, and hence the evaluated specific surface area calculated from using the BET equation can be judged thereafter. The specific surface area and pore size distribution on noncarbonated and well-carbonated cement mortar are evaluated from measured sorption characteristics in paper 7. The assumptions behind the BET theory are described in a more detailed manner in report III:1 than in section 3.5.2. In report III:1, also, an extensive investigation of thermodynamic relations during sorption is performed for a certain choice of constitutive assumptions for the water vapor and the adsorbate. This investigation resulted in an expression for the 'thermodynamic' pressure in the adsorbate.

In section 3.3.2 a multicomponent model based on the so-called mixture theory is described. This model accounts for diffusion and binding/leaching of different kinds of ions present in the pore solution in cement based materials. The effects of positively and negatively charged ions on the diffusion behavior of the individual ion types are included by introducing the so-called electric potential for the mixture of ions in a pore solution. Further, the influence of the moisture content and moisture flow are introduced in the model by identifying the effect of the change of concentration of ions due to a change in moisture content, and by considering convective flow of ions caused by liquid water flow in a pore system. The model presented in section 3.3.2 of this introduction is used in different simplified versions in report I:1-3 and paper 1. In these papers the model is fitted against experimentally obtained chloride profiles for given exposure conditions. The effect of the diffusion of chlorides is compared to porosities of the tested concrete qualities. The experimental methods and their theoretical background described in this introduction can be used to quantify the model described in section 3.3.2. The preliminary result from the established model with its governed equations for the different ion types and for the water content in material suggests that the major experimental work should be directed toward the description of the binding/leaching behavior of different types of ions. One of the main reasons for obtaining this conclusion is that the model assumes that the ion diffusion and the ion mobility, for different types of ions, in bulk water can be

scaled with one single number. This scaling accounts for the porosity, water content and shape of a pore system. All ions present in the pore solution are assumed to be affected by this tortuosity in an identical manner. This becomes an adequate assumption because the diffusion and binding/leaching behavior are treated with separate constitutive assumptions not directly coupled to each other. The tortuosity factor valid for all different types of ions present in the pore solution of certain concrete qualities is estimated from the model and experiments described in reports I:1-3.

At the end of this introduction, i.e. in section 4 and 5, short resume's of the content of the reports and papers included in this thesis are presented. References to the content in previous sections of this introduction are included in order to put the different reports and papers in a clear context.

3 Introductory background

3.1 A short description of concrete

In order to understand the degradation mechanisms of concrete, the chemical composition of the cement used must be considered. Concrete is a mixture of cement (binder), water, aggregate and small amounts of chemical admixtures. The cement consists of grained cement clinker which is produced by heating limestone and minerals like clay, rich in CaO, SiO_2, Al_2O_3 and Fe_2O_3, to about 1500 °C. The major chemical compounds formed in the cement kiln are (*i*) tricalcium silicate $3CaO{\cdot}SiO_2$ (alite, C_3S (shorthand notation)), (*ii*) dicalcium silicate $2CaO{\cdot}SiO_2$ (belite, C_2S), (*iii*) tricalcium aluminate $3CaO{\cdot}Al_2O_3$ (celite, C_3A) and (*iv*) tetracalcium alumino-ferrite $2CaO{\cdot}Al_2O_3{\cdot}Fe_2O_3$ (ferrite, C_4AF). Minor compounds are MgO, free CaO, and alkali sulfates.

The chemical reaction between mixing water and cement is referred to as hydration. A substantial part of the hydration reactions is completed already during one day; the reactions continue, however, at a slow rate for a very long time. The hydration process can be divided into five different stages [1]: (*i*) initial hydrolysis, which involves early rapid dissolutions of ions, (*ii*) induction period, which involves a slow nucleation controlled dissolution of ions, (*iii*) acceleration, the rapid chemically controlled initial formation of hydration products, (*iv*) deceleration, continued formation of hydration products due to chemical and diffusion controlled processes; this stage determines the rate of early strength gain, (*v*) steady state, slow formation of hydration products due to diffusion controlled processes.

The calcium silicates, i.e. $3CaO{\cdot}SiO_2$ and $2CaO{\cdot}SiO_2$ react with water to form Calcium-Silicate-Hydrate (C-S-H), i.e. the so called cement gel, and calcium hydroxide. The two reactions are stoichiometrically very similar and can be written as

$$2\,(3CaO \cdot SiO_2) + 7H_2O \rightarrow 3CaO \cdot 2SiO_2 \cdot 4H_2O + 3Ca\,(OH)_2 \qquad (1)$$

and

$$2\,(2CaO \cdot SiO_2) + 5H_2O \rightarrow 3CaO \cdot 2SiO_2 \cdot 4H_2O + Ca\,(OH)_2 \qquad (2)$$

The formed solid gel $3CaO{\cdot}2SiO_2 \cdot 4H_2O$ is only approximative and can vary over a quite wide range [2]. The gel is poorly crystalline material which

consists of extremely small particles in the range of 1μm. The formed calcium hydroxide $Ca(OH)_2$ is a crystalline material with a fixed composition. The major difference in the hydration of tricalcium silicate and dicalcium silicate is the heat of formation, in which the latter evolve approximately half the heat as compared with tricalcium silicate.

The tricalcium aluminate reacts with water in the presence of a plentiful supply of gypsum, $CaO{\cdot}SO_3 \cdot 2H_2O$, to form ettringite, as

$$\begin{aligned} & 3CaO \cdot Al_2O_3 + 3\,(CaO \cdot SO_3 \cdot 2H_2O) \\ +26H_2O \;\rightarrow\; & 6CaO \cdot Al_2O_3 \cdot 3SO_3 \cdot 32H_2O \end{aligned} \tag{3}$$

When the concentration of sulfate ions in solution drops, the ettringite is no longer stable and continues to react with tricalcium aluminate and water to form monosulfate $3\,(4CaO \cdot Al_2O_3 \cdot SO_3 \cdot 12H_2O)$, as

$$\begin{aligned} & 2\,(3CaO \cdot Al_2O_3) + 6CaO \cdot Al_2O_3 \cdot 3SO_3 \cdot 32H_2O \\ +4H_2O \;\rightarrow\; & 3\,(4CaO \cdot Al_2O_3 \cdot SO_3 \cdot 12H_2O) \end{aligned} \tag{4}$$

The hydration of $3CaO{\cdot}Al_2O_3$ is slowed down as ettringite creates a diffusion barrier around $3CaO{\cdot}Al_2O_3$. The barrier is broken down when ettringite is converted to monosulfate, which results in the hydration of $3CaO{\cdot}Al_2O_3$ becoming rapid again. The heat of hydration of tricalcium aluminate is much higher than the calcium silicate hydration heat.

When not adding gypsum to cement the hydration of $3CaO{\cdot}Al_2O_3$ a rapid formation of calcium aluminate hydrates takes place, as

$$\begin{aligned} & (3CaO \cdot Al_2O_3) + \\ 21H_2O \;\rightarrow\; & 4CaO \cdot Al_2O_3 \cdot 13H_2O + 2CaO \cdot Al_2O_3 \cdot 8H_2O \end{aligned} \tag{5}$$

The two types of calcium aluminate hydrates are closely related structurally to monosulfate. The products are, however not stable and react with each other and form hydrogarnet $3CaO{\cdot}Al_2O_3 \cdot 6H_2O$ and water. The formation of hydrogarnet is unwanted as it may cause a so-called flash set, which means that the cement becomes stiff too early. The molar ratio between gypsum and tricalcium aluminate in cement very much determines the composition of the hydration products. When the ratio $CaO{\cdot}SO_3 \cdot 2H_2O/3CaO{\cdot}Al_2O_3$ is higher than approximately 3 only ettringite is formed; ratios between about 3 and 1 give ettringite and monosulfate, and values close to zero give hydrogarnet.

When monosulfate is brought into contact with a new source of sulfate ions, then ettringite can be formed again, which can cause damage in the microstructure of cement-based materials. Therefore, cements having low contents of $3CaO{\cdot}Al_2O_3$ are used in environments where sulfate ions are present.

The reaction of the ferrite phase $2CaO{\cdot}Al_2O_3{\cdot}Fe_2O_3$ can be described with the same type of reaction sequence as for tricalcium aluminate in the presence of gypsum. The reaction is, however, slower and evolve less heat; furthermore, the gypsum retards the ferrite reaction more drastically as compared to the tricalcium aluminate reaction. Moreover, the hydration rate becomes slower when the iron content in cement increases.

The composition of an ordinary Portland cement (OPC) consists of approximately 55 wt. % tricalcium silicate $3CaO{\cdot}SiO_2$, 20 wt. % dicalcium silicate $2CaO{\cdot}SiO_2$, 12 wt. % tricalcium aluminate $3CaO{\cdot}Al_2O_3$ and 9 wt. % tetracalcium alumino-ferrite $2CaO{\cdot}Al_2O_3{\cdot}Fe_2O_3$. A rapid hardening OPC cement has sometimes substantially higher content of tricalcium silicate as compared to normal hardening OPC. However, a rapid hardening cement can also be obtained by grinding the normal clinker to a higher specific surface area. A low heat cement (low heat of hydration) is obtained by a lower content of tricalcium silicate and a higher content of dicalcium silicate as compared to the composition of OPC. In the so-called sulfate resistant Portland cement, the content of tricalcium aluminate is kept below about 3.5 wt. %.

The use of pozzolans together with pure cement is very common. The pozzolans most used are ground granulated blast furnace slag, silica fume, which is a by-product of the production of silicon or silicon alloys by reducing quartz in an electrical furnace, and fly ash which is the inorganic residue that remains after powdered coal has been burned and is trapped by electrostatic precipitators. Silica fume contains approximately 85-95 wt. % amorphous SiO_2 and the particle size is typically in the range of 0.01-1μm. Fly ash contains 50-60 wt. % amorphous SiO_2 and the particle size is in the range of 1-100μm [3]. The pozzolans react with the calcium hydroxide formed from the cement hydration to form new cement gel according to the principal reaction

$$Ca(OH)_2 + SiO_2 \rightarrow CaO \cdot 2SiO_2 \cdot H_2O \qquad (6)$$

As for the cement, the particle size of pozzolans is one of the factors determining the reactivity with water. The smaller the particle size, the faster

the hydration. Pozzolans with small particle size improve the workability of the fresh concrete without an undue increase in the water demand. When the pozzolan is mixed with Portland cement, it will react with the calcium hydroxide formed during hydration. The effect is then to increase the proportion of cement gel in the hydrated paste at the expense of calcium hydroxide. The cement gel content in hardened concrete is the main factor contributing to strength; therefore pozzolans together with cement are almost always used in high strength concrete.

Besides the mineral admixtures in concrete, such as pozzolans, chemical admixtures are often used to improve certain properties. Chemical admixtures can be divided into four different groups, *(i)* water-reducing admixtures, *(ii)* retarding admixtures, *(iii)* accelerating admixtures and *(iv)* air-entraining agents.

The water-reducing admixtures are added to fresh concrete in order to keep particles from flocculating. If too much water is tied up in agglomerations and/or being adsorbed on solid surfaces, less water is available to reduce the viscosity of the fresh paste and hence of the concrete. Molecules of the water-reducing admixtures interact with the cement particles, water and aggregates in a way that makes the particles repel each other due to residual charges. The effect is that particles remain fully dispersed in the paste and less water is involved in agglomerations. The use of water-reducing admixtures thus makes mixtures containing small quantities of water in relation to cement have the desired properties in terms of fluidity and homogeneity of the fresh concrete. Small content of mixing water in relation to cement content, i.e. low water to cement ratios, is desirable since it increases the strength and the impermeability of hardened concrete. Three categories based on the general active ingredients of water-reducing admixtures are (*i*) salts and derivatives of lignosulfonates, (*ii*) salts and derivatives of hydroxy-carboxylic acids, and (*iii*) polymetric material. Most conventional admixtures achieve water reductions of 5-10%; with newer admixtures called superplasticizers a reduction of 15-30% can be achieved while still obtaining the desired workability of the fresh concrete. Typically 0.5-2.0 percent of active solid components in superplasticizers by weight of cement is used. High contents of water-reducing admixtures should not be used, since it may effect the formed calcium-silicate-hydrate products in a negative manner.

Retarding admixtures can be used whenever it is desirable to offset the effects of high temperatures, due to hydration, which decrease setting times. The admixture can be divided into four groups based on the chemical com-

position, (*i*) lignosulfonic acids and their salts, (*ii*) hydroxylic acids and their salts, (*iii*) sugars and their derivatives, and (*iv*) inorganic salts. It is observed that categories (*i*) and (*ii*) also possess water-reducing properties. Research on the effect of retarders has shown that they slow down the rate of early hydration of tricalcium silicate. One hypothesis is that retardation arises from adsorption on the hydration products.

Accelerating admixtures are beneficial during winter concreting by partially overcoming the slower rate of hydration caused by low temperatures and shortening the period for which protection against damage by freezing is required. Most soluble inorganic salts will accelerate the setting and hardening of concrete to some degree, with calcium salts being most effective. One of the most effective accelerators is calcium chloride whose use, however, should be avoided since it increases the rate of corrosion of metals embedded in concrete.

Air-entraining agents are used to create air bubbles in the paste of concrete which acts as frost protection. The air content must be in the range of 4 to 8% by volume of concrete to obtain satisfactory action. The air-voids should be small, in the range of 0.05-1.25 mm diameter, and the bubble spacing should not exceed about 0.2 to 0.25 mm. Air entrainment increases the workability of an otherwise similar concrete. This allows the water to cement ratio to be decreased and can, therefore, partly or wholly offset the loss in strength arising from the presence of air voids. Air-entraining agents can be compounds such as sodium salts of fatty or alkyl aryl sulfonic acids.

Aggregates generally occupy about 70 to 80% of the volume of concrete and can therefore be expected to have an important influence on its properties. The porosity of the aggregate should be very low, i.e. in the range of 0-1%. Higher porosities of the aggregate should be avoided since they lower the strength, and increase the risk of frost damage. Further, aggregates that are inert with respect to chemical reactions with the paste should be chosen. The particle-size distribution or grading of an aggregate supply is an important characteristic because it determines the paste requirement for a workable concrete.

At nearly all conditions, pores of hardened concrete contain liquid water. This water, referred to as the pore solution, contains different types of ions depending on the composition of the solid hydration products in contact with the pore water and on ions penetrating the concrete from outside. The pH-value in pore solutions is generally very high , i.e. in the range of 13-14. The concentrations of K^+, Na^+ and OH^- in the pore solution of an ordinary

Portland cement (OPC) concrete with a water to cement ratio around 0.40 are typically 750, 120 and 860 mmol/l, respectively. Other ions such as Ca^{2+} also exist in the pore solution in significant concentrations. A sulfate resistant Portland cement (SRPC) concrete, which contains about half of the quantity of alkali sulfates and less tricalcium aluminate as compared to an OPC based concrete, with a water to cement ratio around 0.40, has typically 450, 40 and 480 mmol/l of the ions K^+, Na^+ and OH^- in the pore solution, respectively. Adding pozzolans to cement significantly lowers the concentrations of mainly K^+ and OH^- in the pore solution of a hardened concrete.

The total porosity of fully hydrated 'standard' cement concrete depends mainly on the cement content and the water to cement ratio. As an example, in a concrete with the water to cement ratio 1 and the cement content 175 kg/m^3 without air-entrainment, the total porosity is in the range of 0.16-0.17, and for the water to cement ratio 0.5 and the cement content 370 kg/m^3 the corresponding value is in the range 0.13-0.14. Additional contribution to the porosity must be considered when using air-entraining agents or/and when the aggregate used has a significant porosity. The shape of the porosity in material is such that vapor in the air-filled space can penetrate into the material at a slow rate. In the same manner ions dissolved in a pore solution can penetrate through the pore system.

The cement gel itself has a very high specific surface area. Using the BET-equation on sorption measurements with water vapor, the approximative value of 195 m^2/g is obtained for cement paste with the water to cement ratio 0.5. Using a plate shaped geometrical model and assuming that the gel porosity is 0.28 and that the compact density of gel is 2460 kg/m^3, the mean pore size in gel can be estimated to be about 13 Å and the mean thickness of gel 'plates' to be about 32 Å. The microstructure in terms of the specific surface area is an important property determining the extent and rate of mass exchange of ions in a pore solution and ions involved in the solid components of the hydrated cement paste.

3.2 A short review of mechanisms of degradation of reinforced concrete structures

The reports and papers presented in this work deal with only a few of the service life related problems of concrete structures. The main content to be presented is related to the description of some of the most common types of ions in pore solutions and properties of solid constituents in cement-based materials.

3.2.1 Chloride penetration and reinforcement corrosion

Concrete structures in marine environments or constructions subjected to de-icing salt agents suffer a considerable risk of being degraded due to reinforcement corrosion. The penetration rate of chloride ions into concrete depends on, among other things, the water to cement ratio, cement and pozzolan content and the moisture condition in the structure. The corrosion rate is very much related to the condition of the pore solution near the reinforcement bars, mainly in terms of the concentrations of chloride ions and hydroxide ions. The oxidation reaction in the corrosion process involves the dissolution of iron in the pore water near the steel, written as

$$\mathrm{Fe(s)} \longrightarrow \mathrm{Fe^{2+}(aq)} + 2e^- \quad \text{(at the anode)} \tag{7}$$

where e^- denotes an electron. This reaction may only occur if the depassivation of the steel has been induced, for example by the presence of chloride ions in the pore solution at a sufficiently high concentration (presumably caused by breaking the oxide film on the steel surface) or/and a decrease in the basicity. The threshold chloride concentration required for onset of corrosion has not been fully clarified. It probably depends on such factors as the OH^- concentration of the pore fluid surrounding the bar and the O_2-concentration around the bar, and factors that affect the electrical potential of the steel [4].

Incoming electrons from the steel bar at the cathodic area form hydroxide ions in the presence of water. The oxygen reduction reaction is

$$\mathrm{O_2(aq)} + 2\mathrm{H_2O} + 4e^- \longrightarrow 4\mathrm{OH^-(aq)} \quad \text{(at the cathode)} \tag{8}$$

Apparently, the rate of the induced reaction is very much determined by the concentration of the hydroxide ions in the pore solution near the steel.

The hydroxide ions that are liberated in the cathode area are balanced by a reaction in the anodic region, to form ferrous hydroxide, i.e.

$$Fe^{2+}(aq) + 2OH^{-}(aq) \longrightarrow 2Fe(OH)_2(s) \quad \text{(anode)} \tag{9}$$

Since the hydroxide ions liberated at the cathode can be transferred through the electrolyte, in this case the pore solution, the flow properties of the hydroxide ions in the pore solution near or at the interface between the concrete and the steel are of importance. The ferrous hydroxide will, furthermore, react with available dissolved oxygen or oxygen in its gaseous phase to form hydrated red rust $Fe(OH)_3$:

$$4Fe(OH)_2(s) + O_2(aq \text{ or } g) + 2H_2O \longrightarrow 4Fe(OH)_3(s) \quad \text{(anode)} \tag{10}$$

where, again, the availability of oxygen and liquid water are important for the reaction rate. The expansion of the corrosion products induces cracks in the concrete surrounding the bars.

3.2.2 Carbonation of hydration products in concrete

Carbon dioxide in air penetrates the concrete pore system and dissolves in the pore solution. The carbonic acid formed will react with solid products such as calcium-hydroxide. Depending on the cement type used, the porosity can either decrease or increase. The final result of the several steps through which the calcium carbonate is formed can be described simply by the following reaction:

$$CO_2(aq) + Ca^{2+}(aq) + 2OH^{-}(aq) \longrightarrow CaCO_3(s) + H_2O \tag{11}$$

Carbonation reduces the hydroxide ion concentration in the pore solution, which is a negative factor with regard to reinforcement corrosion since the steel surface becomes de-passivated.

3.2.3 Leaching of hydroxide from a pore solution

The leaching process slowly breaks down the solid calcium hydroxide and cement gel in the hydration products of concrete. The leaching process is always active when concrete is in contact with water containing low concentrations of hydroxide ions. The leaching can simply be described as

$$Ca(OH)_2(s) \longrightarrow Ca^{2+}(aq) + 2OH^{-}(aq) \tag{12}$$

The hydroxide leaching from the pore solution in concrete can be considerably high when external water pressures acts on a construction such as in concrete dams, e.g. see [5].

3.2.4 Sulfate Attack

Concrete in contact with sulfate ions will suffer a risk of being degraded. Sulfate attack is due to sulfate ions from external water penetrating the concrete; the sulfate ions react mainly with the hydration products based on tricalcium-aluminate. The products formed, such as gypsum and ettringite, make the material expand due to microcracking. Cements low in aluminate are regarded as being sulfate resistant. One of the main reactions valid during sulfate attack, causing ettringite formation, is

$$\begin{aligned} & & 4CaO \cdot Al_2O_3 \cdot SO_3 \cdot 12H_2O + 2\,(CaO \cdot SO_3 \cdot 2H_2O) \quad (13) \\ +2H_2O & \longrightarrow & 6CaO \cdot Al_2O_3 \cdot 3SO_3 \cdot 32H_2O \end{aligned}$$

This is accomplished by a very large increase in solid volume, which causes volume expansion within paste and which generates accompanying internal stresses and ultimately leads to cracking.

3.2.5 Paste-aggregate reactions

The most common case of paste-aggregate reaction is the alkali-silica reaction which is caused by aggregates containing amorph SiO_2, which is sensitive for reaction with the ions in the alkali rich pore solution. A thin zone of reaction products is formed around the aggregates, the so-called alkali-silica gel. The alkali-silica gel formed expands when exposed to high moisture conditions. The damage caused by alkali-silica reaction is sometimes observed as pop-outs at the concrete surface. Destructive expansion also occurs in concretes made with some aggregates containing dolomite, which reacts with hydroxide ions in a pore solution.

3.2.6 Freeze thaw damage

Due to the expansion of water in a pore system when frozen, the concrete can be damaged. The damage depends on the degree of water saturation of the pore system, the amount of air bubbles in the material and the spacing between them, e.g. see [6]. Often factors like the water to cement ratio and

the aggregate porosity also plays a significant role. Special attention must therefore be paid to concrete constructions used in cold moist climates.

3.2.7 Salt frost scaling

Special types of damage in concrete can occur if freezing is active when simultaneously having a salt solution present at the surface of the material. A typical case is when using de-icing salt agents at low temperatures. The observed damage during this situation is that thin flakes at the concrete surface are spalled off. The phenomenon can be explained by the fact that chlorides penetrate the concrete slowly as compared with the temperature decrease in the material. Since the salt in a pore solution lowers the freeze point temperature, the first ice is formed at a depth which is greater than the depth at which a significant salt concentration can be detected. The changes in expansion at the surface and just beneath the surface of the material makes thin flakes spall off, see [7]. Other mechanisms for the salt frost scaling has also been proposed, e.g. see [7].

3.2.8 Degradation caused by mechanical loads

Effects on concrete structures due to dead and variable loads include for example, cracking, creep and wear. The mechanically induced damages can be accelerated when constructions are simultaneously subjected to other destruction mechanisms such the ones mentioned above.

3.2.9 Damage induced by thermal effects and moisture conditions

Environmentally induced strains caused by a change in temperature and/or moisture condition can cause damage often visible in the form of cracks. Such damage can be avoided by using construction joints and a proper arrangement of the reinforcement bars. A model based on fracture mechanics has been established describing the effect of moisture and temperature changes on concrete [8].

3.2.10 Durability conditions of concrete structures related to the production stage

If the heat of hydration in heavy constructions is not properly accounted for, the risk of obtaining cracks is substantial. Low heat cements and/or cooling

systems are often used. Drying of the concrete during the early hydration period can cause damage. Insufficient compaction during casting is a common problem causing unwanted nonhomogeneities in the structure. Design issues such as avoiding accumulation of water during construction, and placing the reinforcement bars at sufficient depths from surfaces, should be considered.

3.3 Chloride ingress in concrete

3.3.1 Transport of ions in the pore solution of hardened concrete

Nearly all deterioration processes of reinforced concrete structures are associated with the amount of pore liquid and the condition of the pore solution in terms of concentrations of different types of ions, e.g. see previous sections. Therefore it is important to try to understand the underlying mechanisms which determine the changes of concentrations in pore solutions due to diffusion and chemical reactions. Some of the most common mechanisms affecting the condition of the pore solution are listed below

1. *Concentration gradient driven diffusion*: The most important properties affecting the diffusion of ions in pore solution of concrete are porosity and the degree of water saturation in pores, shape of pore system and presence of microcracks and other nonhomogeneities. One of the 'forces' contributing to a mass density flow of ions dissolved in pore solution is the concentration gradient. The diffusion resistance of the ions increases when the concentration of liquid water in a pore system decreases. Diffusion of vapors in the air filled space of concrete, in which oxygen and carbon dioxide are most important, are affected by the liquid water concentration in the opposite direction as compared with the dissolved ions in a pore solution.

2. *Binding*: The physical or chemical binding of ions, from external sources, onto inner material surfaces in concrete, such as chloride binding, are dependent on many different factors. Properties affecting binding are the specific surface area of solid hydration products, the chemical composition of solid hydration products, and the composition of the pore solution. The binding of ions from pore solution should be incorporated into models dealing with diffusion, since the process changes the concentration in the pore solution.

3. *Leaching:* Describes the process of solids being broken down and dissolved in the pore solution. The most common leaching in cement based materials is the decalcification of the solid calcium hydroxide in concrete, i.e. the dissolution of calcium ions and hydroxide ions into the pore solution. The conditions in both the pore solution and in the solid components of concrete are changed.

4. *Convection of ions*: Capillary suction of external water can force dissolved ions in a pore solution to be moved in the direction of the capillary flow. Drying of concrete surfaces may force ions to be moved in the direction of the surface. The drying is however mostly due to movement of water vapor in the air filled pore space not affecting the convective flow. Hence a correct description of the flow characteristics of the liquid water phase becomes essential when including convection of ions dissolved in a pore solution.

5. *Diffusion of ions induced by internal dielectric effects:* As pointed out in previous sections, the pore solution in contact with solid hydration products in concrete always contains significant concentrations of different types of ions. It can be postulated that different ions, of positive and negative charge, must diffuse in the pore system in a way that the net charge in every material point and at every time level is close to zero. This means that not only the concentration gradient and the convective driven flow of ions should be considered, but also a force related to the charge character of the mixture of all different types of ions present in a representative volume of the pore solution.

6. *Water saturation*: The degree of water saturation not only determines the diffusion resistance of ions dissolved in a pore solution. The drying process means that the ion concentration in the pore solution is increased, and that an increase of water content in material results in the pore solution becoming more dilute. This effect can be modelled in a direct manner if relating the ion concentration in pore solution to the volume of pore solution and not to the total volume of material.

7. *Diffusion caused be external electrical forces induced by reinforcement corrosion*: A corrosion current is active during the propagation stage of reinforcement corrosion. The induced electrical field will affect ions in a pore solution located in domains surrounding the corrosion zone including both the cathodic and anodic areas. All different kinds of ions present in the pore solution within the corrosion zone will, in this case, be subjected to a force making the diffusion behavior markedly different from normal situations not including active corrosion.

8. *Clogging of pores due to hydration and crystallization:* During the early stage of concrete, properties such as porosity and specific surface area

are significantly and rapidly changed with time. The diffusion behavior of ions during this period is, therefore, also affected. Even for well cured concrete the binding and leaching process can affect the pore structure in a way that the diffusion resistance in a pore solution is affected.

3.3.2 Diffusion of a mixture of different types of ions coupled to moisture transport in concrete

Most concrete constructions subjected to harmful ions such as chlorides, sulfates and carbonic acid are also exposed to variations in moisture content. Phenomena such as capillary suction and drying will affect the diffusion of different types of ions dissolved in a pore solution. A stringent model of this problem should result in one equation for each type of ion appearing in a pore solution, one equation describing the moisture transport and one equation for each solid component being formed from ions in the pore solution or being dissolved into the pore solution from solid components.

The basic concept behind the so-called mixture theory will be used, e.g. see [9], in order to establish a model describing diffusion of a mixture of different types of ions in a pore solution of concrete, and its couplings to the moisture condition and moisture flow. Each constituent is assigned a mass density concentration. The mass density concentration of the $i = 1, ..., \Re$ dissolved ions considered in pore solution will be denoted ρ_i^p (kg/m^3) and the $s = 1, ..., \Im$ solid precipitated combinations of ions in pore solution will be denoted ρ_s^p. The $h = 1, ..., \aleph$ solid components of the concrete will be denoted ρ_h^c and the mass density concentration of liquid water in the material volume will be denoted ρ_w^p. The total mass density of the mixture ρ is the sum of all constituents. Two phases will be considered, the pore solution phase p and the solid phase of the concrete c. Reactions within and between the phases will be considered in the general case. The only balance principle that will be considered are the mass balance equations for the constituents, the two phases and the whole mixture, i.e. the momentum balance equation, energy balance equation and the second axiom of thermodynamics are ignored in this presentation.

It will be seen that the complexity of the problem considered grows drastically as compared to, for example, the isothermal moisture transport problem which only includes one mass balance principle and one constitutive equation, e.g. see section 3.4.1.

The mass density concentration of solid component phase ρ^c, i.e. the 'dry'

concrete density, is the sum of the $\aleph$ number of individual solid constituents, i.e.

$$\rho^c = \sum_{h=1}^{\aleph} \rho_h^c \tag{14}$$

where ρ_h^c is the mass density concentration of the h:th solid component.

The mass density concentration of the pore solution phase ρ^p is the sum of the $\Re$ number of dissolved ion constituents, the sum of the $\Im$ number of solid precipitated combinations of ions and the water itself, i.e.

$$\rho^p = \sum_{i=1}^{\Re} \rho_i^p + \sum_{s=1}^{\Im} \rho_s^p + \rho_w^p \tag{15}$$

where ρ_i^p is the mass density concentration of the i:th dissolved ion constituent, ρ_s^p is the mass density concentration of the s:th precipitated constituent in pore water phase and ρ_w^p is the mass density concentration of the 'pure' water in material. The total mass density concentration of the mixture ρ is

$$\rho = \rho^c + \rho^p = \sum_{h=1}^{\aleph} \rho_h^c + \sum_{i=1}^{\Re} \rho_i^p + \sum_{s=1}^{\Im} \rho_s^p + \rho_w^p \tag{16}$$

The mean velocity of the pore solution phase $\dot{x}^p$ is defined as the mass weighted average of individual constituent velocities $\acute{x}_i^p$ (m/s), $\acute{x}_s^p$ and $\acute{x}_w^p$, i.e.

$$\dot{x}^p = \frac{1}{\rho^p} \sum_{i=1}^{\Re} \rho_i^p \acute{x}_i^p + \frac{1}{\rho^p} \sum_{s=1}^{\Im} \rho_s^p \acute{x}_s^p + \frac{\rho_w^p \acute{x}_w^p}{\rho^p} \tag{17}$$

The mixture velocity of the solid phase $\dot{x}^c$ is the mass weighted average of individual solid constituent velocities $\acute{x}_h^c$, i.e.

$$\dot{x}^c = \frac{1}{\rho^c} \sum_{h=1}^{\aleph} \rho_h^c \acute{x}_h^c \tag{18}$$

The velocity of the whole mixture $\dot{x}$ is defined to be the sum of $\dot{x}^p$ and $\dot{x}^c$, that is

$$\dot{x} = \frac{1}{\rho} \sum_{i=1}^{\Re} \rho_i^p \acute{x}_i + \frac{1}{\rho} \sum_{s=1}^{\Im} \rho_s^p \acute{x}_s + \frac{\rho_w^p \acute{x}_w}{\rho} + \frac{1}{\rho} \sum_{h=1}^{\aleph} \rho_h^c \acute{x}_h \tag{19}$$

In a general case where $\acute{x}_h^c$ is different from zero, the mass balance principle for the $\aleph$ number of solid constituents of the concrete phase c can be written as

$$\frac{\partial \rho_h^c}{\partial t} = -\frac{\partial \left(\rho_h^c \dot{x}_h^c\right)}{\partial x} + \hat{c}_h^c + \hat{r}_h^c; \qquad h = 1, ..., \aleph \tag{20}$$

where $\hat{c}_h^c$ is the gain of mass from all $\aleph - 1$ number of solid constituents present in phase c. The term $\hat{r}_h^c$ is the gain of mass to the h:th constituent from the $\Re + \Im + 1$ number of constituents building up the pore solution phase p.

The postulate for the mass balance for the solid phase c is

$$\frac{\partial \rho^c}{\partial t} = -\frac{\partial \left(\rho^c \dot{x}^c\right)}{\partial x} + \hat{r}^c \tag{21}$$

where $\hat{r}^c$ is the total gain of mass to the solid concrete phase from the pore solution phase, i.e. $\hat{r}^c$ is related to $\hat{r}_h^c$, as

$$\hat{r}^c = \sum_{h=1}^{\aleph} \hat{r}_h^c \tag{22}$$

In mixture theory it is postulated that the sum of the constituent balance principles in a phase should be equal to the mass balance equation for the whole phase. Summing the $\aleph$ number of balance principles in (20), therefore, results in

$$\sum_{h=1}^{\aleph} \hat{c}_h^c = 0 \tag{23}$$

where (19), (20), (21) and (22) are used.

The mass balance for the pure water w in the pore solution phase p is the postulate

$$\frac{\partial \rho_w^p}{\partial t} = -\frac{\partial \left(\rho_w^p \dot{x}_w^p\right)}{\partial x} + \hat{c}_w^p + \hat{r}_w^p \tag{24}$$

where $\hat{c}_w^p$ and $\hat{r}_w^p$ are the gain of mass to the w constituents from constituents within phase p and from phase c, respectively.

The mass balance principle for the different types of dissolved ions in pore solution is

$$\frac{\partial \rho_i^p}{\partial t} = -\frac{\partial \left(\rho_i^p \dot{x}_i^p\right)}{\partial x} + \hat{c}_i^p + \hat{r}_i^p; \qquad i = 1, ..., \Re \tag{25}$$

where $\hat{c}_i^p$ is the mass gain to the dissolved ion constituent i from the $\Im$ number of solid constituents in a pore solution, i.e. in phase p. The property $\hat{r}_i^p$ is the mass gain to the dissolved ion constituent i from the solid phase c.

The mass balance principle for the solid precipitated neutral combinations of ions in pore solution is

$$\frac{\partial \rho_s^p}{\partial t} = -\frac{\partial \left(\rho_s^p \dot{x}_s^p\right)}{\partial x} + \hat{c}_s^p + \hat{r}_s^p; \qquad s = 1, ..., \Im \tag{26}$$

where $\hat{c}_s^p$ is the mass gain to the solid constituent s in the pore solution from the i number of dissolved ions also present in the pore solution. The term $\hat{r}_s^p$ is the mass gain to the solid constituent s in the pore solution, i.e. in phase p, from the solid phase c.

The mass balance for the whole pore solution phase p is the postulate

$$\frac{\partial \rho^p}{\partial t} = -\frac{\partial \left(\rho^p \dot{x}^p\right)}{\partial x} + \hat{r}^p \tag{27}$$

where $\hat{r}^p$ is the total gain of mass from the solid phase c, i.e.

$$\hat{r}^p = \sum_{i=1}^{\Re} \hat{r}_i^p + \sum_{c=1}^{\Im} \hat{r}_s^p + \hat{r}_w^p \tag{28}$$

The sum of equation (24), the $\Re$ number of equations in (25) and the $\Im$ number of equations in (26), should result in satisfying condition

$$\sum_{i=1}^{\Re} \hat{c}_i^p + \sum_{c=1}^{\Im} \hat{c}_s^p + \hat{c}_w = 0, \tag{29}$$

since it is postulated that equation (27) is the sum of the constituent equations in phase p.

The postulated mass balance for the whole mixture, including both the pore solution phase p and the solid phase c, is

$$\frac{\partial \rho}{\partial t} = -\frac{\partial \left(\rho \dot{x}\right)}{\partial x} \tag{30}$$

Summation of the mass balance equations for the c and p phases, i.e. equation (20) and (27), results in the relation

$$\hat{r}^p + \hat{r}^c = 0 \tag{31}$$

where (17), (18) and (19) are used.

Yet another balance principle will be invoked for the pore solution phase p, the continuity equation for the charge, which is

$$\frac{\partial d^p}{\partial x} = q^p \tag{32}$$

where the electrical displacement field is denoted by d ($\mathrm{C/m^2}$) and the charge density with q ($\mathrm{C/m^3}$). This equation will control the condition of the pore solution in terms of an electrical potential φ. The reason for obtaining an electrical potential in a pore solution is a momentarily unbalancing number of positive and negatively charged dissolved ions in a representative volume being much larger than the size of the ions themselves.

In this application it is convenient to introduce the so-called diffusion velocity, which is the velocity of a constituent in relation to the phase mixture velocity.

$$u_i^p = \acute{x}_i^p - \dot{x}^p \tag{33}$$

$$u_h^c = \acute{x}_h^c - \dot{x}^c \tag{34}$$

It will be explicitly assumed that different dissolved ions in a pore solution cannot react with each other, i.e. the problem will be restricted to a case where precipitation of combinations of ions cannot occur. This means that the mass exchange terms $\hat{c}_i^p(x,t)$, $i = 1, ..., \Re$ are set to zero. The unknown quantities for the $\Re$ number of different types of ions dissolved in the pore solution, therefore, are

$$\rho_i^p(x,t); \quad u_i^p(x,t); \quad r_i^p(x,t); \qquad i = 1, ..., \Re \tag{35}$$

where ρ_i^p is the mass density concentration of an arbitrary type of ion dissolved in the pore solution, u_i^p is the corresponding diffusion velocity, i.e. the velocity of the ion type i in relation to the velocity of the phase mixture, i.e. in relation to $\dot{x}^p$.

For the 'pure' water in a pore solution it will be explicitly assumed that $\hat{c}_w^p(x,t) = 0$. Furthermore it will be assumed that $r_w^p(x,t) = 0$, i.e. effects such as loss of water due to hydration or gain of water due to carbonation will not be included in the model. The unknown properties left for the 'pure' water in the pore solution are

$$\rho_w^p(x,t) \quad \text{and} \quad \acute{x}_w^p(x,t) \tag{36}$$

For the $\Im$ number of solid components in the pore solution phase p, denoted by a subscript s, it will be assumed that the velocities $s = 1, ..., \Im$ are zero, i.e. $\acute{x}_s^p(x,t) = 0$, and that no mass exchanges take place within the phase or between the two phases, i.e. $\hat{c}_s^p(x,t) = 0$ and $r_s^p(x,t) = 0$ for all $s = 1, ..., \Im$ constituents. This means that the mass densities for the precipitated combinations of salts in a pore solution will be entirely given by its initial values. For simplicity these initial values will be set to zero.

The properties of the solid constituents in concrete will be restricted in the sense that the velocities for $\aleph$ number of constituents are set to zero, i.e. $\acute{x}_h^c(x,t) = 0$. Further, no reactions between the $\aleph$ number of solid constituents within the phase c will be included, i.e. $\hat{c}_h^c(x,t) = 0$. The unknown properties of the solid constituents in phase c, therefore, are

$$\rho_h^c(x,t); \qquad r_h^c(x,t); \qquad h = 1, ..., \aleph \tag{37}$$

The unknown properties for the whole mixture, including both phase p and c, are

$$\rho(x,t); \qquad \dot{x}(x,t) \tag{38}$$

where ρ and $\dot{x}$ are defined in (16) and (19).

In order to study the influence of the charge of the different kinds of ions in the pore solution phase on the diffusion behavior, the electrical potential φ^p (V), the electrical displacement field d^p (C/m^2) and the charge density q^p (C/m^3) must be added to the list of unknown properties in the problem studied.

$$\varphi^p(x,t); \qquad d^p(x,t); \qquad q^p(x,t) \tag{39}$$

The number of unknown properties in the reduced problem is $7 + 3\Re + 2\Im$.

With the above assumptions the balance principles for the constituents are simplified. For the solid components in the phase c, one obtains the mass balance equation

$$\frac{\partial \rho_h^c}{\partial t} = \hat{r}_h^c; \qquad h = 1, ..., \aleph \tag{40}$$

The simplified mass balance equation for the pure water constituent becomes

$$\frac{\partial \rho_w^p}{\partial t} = -\frac{\partial (\rho_w^p \acute{x}_w^p)}{\partial x} \tag{41}$$

The mass balance for the $\Re$ number of dissolved ions in the pore solution are

$$\frac{\partial \rho_i^p}{\partial t} = -\frac{\partial \left(\rho_i^p \acute{x}_i^p\right)}{\partial x} + \hat{r}_i^p; \qquad i = 1, ..., \Re \tag{42}$$

The conditions imposed by the mass balance for the whole mixture imply that no net production of mass can take place during mass exchange between the two phases. That is, the mass balance condition

$$\sum_{i=1}^{\Re} \hat{r}_i^p + \sum_{h=1}^{\aleph} \hat{r}_h^c = 0 \tag{43}$$

must hold.

The last balance principle considered is the condition for the electrical potential, which is

$$\frac{\partial d^p}{\partial x} = q^p \tag{44}$$

In the application to be presented it will be of interest to use a mol density concentration definition of the ion constituents dissolved in pore water, instead of the mass density concentration definition. The relation between the mass density concentration ρ_a and the mol density concentration n_i^p (mol/m^3) is

$$\rho_i^p = n_i^p m_i; \tag{45}$$

where m_i (kg/mol) is the mass of one mol of the i:th constituent which is a constant property. By definition (45) the mass balance equation for the ion constituents (42) can be written

$$m_i \frac{\partial n_i^p}{\partial t} = -m_i \frac{\partial \left(n_i^p \acute{x}_i^p\right)}{\partial x} + m_i \hat{n}_i^p; \qquad i = 1, ..., \Re, \tag{46}$$

where the mass gain density to the i:th constituent $\hat{r}_i^p$ is related to the mol gain density $\hat{n}_a$ (mol/(m^{3}s)) as $\hat{n}_i^p = \hat{r}_i^p / m_i$. That is, the mass balance principle for the ion constituents (46) can be written as

$$\frac{\partial n_i^p}{\partial t} = -\frac{\partial \left(n_i^p \acute{x}_i^p\right)}{\partial x} + \hat{n}_i^p; \qquad i = 1, ..., \Re, \tag{47}$$

This equation will be rewritten in yet another way in order to facilitate the description of the diffusion velocities of the different types of dissolved ions. Consider the concentration c_i^p (-) of the ion constituents, defined as

$$c_i^p = \rho_i^p / \rho^p = n_i^p m_i / \rho^p \tag{48}$$

This definition together with equations (33) and (42) can be combined to yield

$$\frac{\partial \left(c_i^p \rho^p\right)}{\partial t} = -\frac{\partial \left(\rho_i^p u_i^p\right)}{\partial x} - \frac{\partial \left(c_i^p \rho^p \dot{x}^p\right)}{\partial x} + \hat{r}_i^p; \qquad i = 1, ..., \Re \tag{49}$$

Partial differentiation of the terms

$$\frac{\partial \left(c_i^p \rho^p\right)}{\partial t} = c_i^p \frac{\partial \rho^p}{\partial t} + \rho^p \frac{\partial c_i^p}{\partial t} \tag{50}$$

and

$$\frac{\partial \left(c_i^p \rho^p \dot{x}^p\right)}{\partial x} = c_i^p \frac{\partial \left(\rho^p \dot{x}^p\right)}{\partial x} + \rho^p \dot{x}^p \frac{\partial c_i^p}{\partial x} \tag{51}$$

makes it possible to write equation (49) as

$$\begin{aligned} c_i^p \left(\frac{\partial \rho^p}{\partial t} + \frac{\partial \left(\rho^p \dot{x}^p\right)}{\partial x} \right) + \rho^p \frac{\partial c_i^p}{\partial t} &= -\frac{\partial \left(\rho_i^p u_i^p\right)}{\partial x} - \\ \rho^p \dot{x}^p \frac{\partial c_i^p}{\partial x} + \hat{r}_i^p; \qquad i &= 1, ..., \Re \end{aligned} \tag{52}$$

The first term on the left-hand side of (52) can be identified by help from the mass balance equation for the phase p, i.e. equation (27), as

$$c_i^p \left(\frac{\partial \rho^p}{\partial t} + \frac{\partial \left(\rho^p \dot{x}^p\right)}{\partial x} \right) = c_i^p \hat{r}^p = c_i^p \sum_{i=1}^{\Re} \hat{r}_i^p \tag{53}$$

where (27) with $\hat{r}_s^p = 0$, for $s = 1, ..., \Im$, and $\hat{r}_w^p = 0$ are used. The equations (52) and (53) combine to yield

$$\rho^p \frac{\partial c_i^p}{\partial t} = -\frac{\partial \left(\rho_i^p u_i^p\right)}{\partial x} - \rho^p \dot{x}^p \frac{\partial c_i^p}{\partial x} + \hat{r}_i^p - \frac{\rho_i^p \sum_{i=1}^{\Re} \hat{r}_i^p}{\rho^p}; \qquad i = 1, ..., \Re \tag{54}$$

Using the mol density concentration, as defined in (45), instead of the concentration c_a, the equation (54) takes the form

$$\begin{aligned} \rho^p m_i \frac{\partial \left(n_i^p / \rho^p\right)}{\partial t} &= -\frac{\partial \left(\rho_i^p u_i^p\right)}{\partial x} - \rho^p m_i \dot{x}^p \frac{\partial \left(n_i^p / \rho^p\right)}{\partial x} + \\ \hat{r}_i^p - \frac{n_i^p \sum_{i=1}^{\Re} m_i \hat{r}_i^p}{\rho^p}; \qquad i &= 1, ..., \Re \end{aligned} \tag{55}$$

Partial differentiation of the term

$$\frac{\partial\left(n_i^p/\rho^p\right)}{\partial x} = \frac{1}{\rho^p}\frac{\partial n_i^p}{\partial x} - \frac{n_i^p}{\left(\rho^p\right)^2}\frac{\partial \rho^p}{\partial x} \tag{56}$$

and

$$\frac{\partial\left(n_i^p/\rho^p\right)}{\partial t} = \frac{1}{\rho^p}\frac{\partial n_i^p}{\partial t} - \frac{n_i^p}{\left(\rho^p\right)^2}\frac{\partial \rho^p}{\partial t} \tag{57}$$

in (55) means that the mass balance equation for the ions dissolved in pore water can be written as

$$\begin{aligned}\frac{\partial n_i^p}{\partial t} - \frac{n_i^p}{\rho^p}\frac{\partial \rho^p}{\partial t} &= -\frac{1}{m_i}\frac{\partial\left(\rho_i^p u_i^p\right)}{\partial x} - \dot{x}^p\frac{\partial n_i^p}{\partial x} + \frac{n_i^p \dot{x}^p}{\rho^p}\frac{\partial \rho^p}{\partial x} + \\ \hat{n}_i^p - \frac{n_i^p \sum_{i=1}^{\Re}\hat{r}_i^p}{\rho^p}; \qquad i &= 1,...,\Re\end{aligned} \tag{58}$$

The assumption that the mass density concentration for the pure water phase is much greater than any of the mass density concentrations of the dissolved ions will be used, i.e.

$$\rho_w^p \gg \rho_{i=1,...\Re}^p; \tag{59}$$

This results in the mean velocity of the pore solution phase $\dot{x}^p$ being approximately equal to the velocity $\acute{x}_w^p$ of the pore solution, i.e. compare with (17). Furthermore, the mass density of the pore solution phase is approximately equal to the mass density of pure water, i.e. the approximation in (59), results in

$$\dot{x}^p \approx \acute{x}_w^p; \quad \rho^p \approx \rho_w^p \tag{60}$$

The approximative version of the balance principle for the ion constituents in pore solution becomes with (60)

$$\begin{aligned}\frac{\partial n_i^p}{\partial t} - \frac{n_i^p}{\rho_w^p}\frac{\partial \rho_w^p}{\partial t} &= -\frac{1}{m_i}\frac{\partial\left(\rho_i^p u_i^p\right)}{\partial x} - \acute{x}_w^p\frac{\partial n_i^p}{\partial x} + \\ \frac{n_i^p \acute{x}_w^p}{\rho_w^p}\frac{\partial \rho_w^p}{\partial x} + \hat{n}_i^p; \qquad i &= 1,...,\Re\end{aligned} \tag{61}$$

for all $\Re$ considered ions. It is noted that the term

$$\frac{n_i^p \sum_{i=1}^{\Re}\hat{r}_i^p}{\rho_w^p} = \frac{\rho_i^p \sum_{i=1}^{\Re}\hat{r}_i^p}{m_i \rho_w^p} \approx 0 \tag{62}$$

in (58), is approximately zero due to the conditions in (60).

Consider the mass balance equation for the pure water constituent, i.e. (41), written as

$$\frac{n_i^p}{\rho_w^p}\frac{\partial \rho_w^p}{\partial t} = -\frac{n_i^p}{\rho_w^p}\frac{\partial\left(\rho_w^p \acute{x}_w^p\right)}{\partial x} \tag{63}$$

i.e.

$$\frac{n_i^p}{\rho_w^p}\frac{\partial \rho_w^p}{\partial t} = -\frac{n_i^p \acute{x}_w^p}{\rho_w^p}\frac{\partial \rho_w^p}{\partial x} - n_i^p \frac{\partial \acute{x}_w^p}{\partial x} \tag{64}$$

This means that the $\Re$ equations in (61) can be written as

$$\frac{\partial n_i^p}{\partial t} = -\frac{1}{m_i}\frac{\partial\left(\rho_i^p u_i^p\right)}{\partial x} - \acute{x}_w^p \frac{\partial n_i^p}{\partial x} - n_i^p \frac{\partial \acute{x}_w^p}{\partial x} + \hat{n}_i^p; \qquad i = 1, ..., \Re \tag{65}$$

The term $n_i^p \partial \acute{x}_w / \partial x$, in equation (65), represents the change in the mass density concentration of ion i in a pore solution due to a change in the mass density concentration of the pore solution caused by drying or capillary suction. To show the meaning of the term $n_i^p \partial \acute{x}_w / \partial x$, consider again the mass balance for the 'pure' water in the pore solution phase, i.e.

$$\frac{\partial \rho_w^p}{\partial t} = -\frac{\partial\left(\rho_w^p \acute{x}_w^p\right)}{\partial x} = -\acute{x}_w^p \frac{\partial \rho_w^p}{\partial x} - \rho_w^p \frac{\partial \acute{x}_w^p}{\partial x} \tag{66}$$

Note that the material derivative of ρ_w^p, denoted $\left(\rho_w^p\right)'$, is the change in mass density concentration related to the motion $\acute{x}_w^p$ given as

$$\left(\rho_w^p\right)' = \frac{\partial \rho_w^p}{\partial t} + \acute{x}_w^p \frac{\partial \rho_w^p}{\partial x} \tag{67}$$

That is, by combining (66) and (67), the mass balance equation using the material description becomes

$$\left(\rho_w^p\right)' = -\rho_w^p \frac{\partial \acute{x}_w^p}{\partial x} \tag{68}$$

This means that the ratio between the change in mass density concentration of the pore water, following its own motion, and the actual mass density concentration is proportional to $\partial \acute{x}_w^p / \partial x$, i.e.

$$\frac{\left(\rho_w^p\right)'}{\rho_w^p} = -\frac{\partial \acute{x}_w^p}{\partial x} \tag{69}$$

Hence term $n_i^p \partial \acute{x}_w / \partial x = n_i^p \left(\rho_w^p\right)' / \rho_w$ is the absolute change of the mass concentration of ion i dissolved in a pore solution, following the motion of the pore water.

Next, consider the constitutive relations for the constituents. The velocity of the pore water in material is the assumption

$$\acute{x}_w^p = -\frac{D_w^p\left(\rho_w^p\right)}{\rho_w^p} \frac{\partial \rho_w^p}{\partial x} \tag{70}$$

where $D_w^p\left(\rho_w^p\right)$ is the nonlinear material parameter relating the gradient of the mass density concentration of water in pores with the velocity $\acute{x}_w^p$. The experimental methods described in sections 3.4.4 and 3.5.1, together with either of the evaluation methods described in sections 3.4.1 or 3.4.2 can be used to obtain the function $D_w^p\left(\rho_w^p\right)$.

The assumptions for the diffusion velocity flows for the $\Re$ considered types of ions in a pore solution are

$$\rho_i^p u_i^p = -\tilde{D}_i^p\left(\rho_w^p\right) m_i \frac{\partial n_i}{\partial x} - \tilde{A}_i^p\left(\rho_w^p\right) m_i v_i n_i^p \frac{\partial \varphi}{\partial x}; \qquad i = 1, ..., \Re \tag{71}$$

where $\tilde{D}_i^p\left(\rho_w\right)$ (m^2/s) is the diffusion parameter for ion type i in the pore system which is assumed to be dependent on the moisture condition ρ_w. The property $\tilde{A}_i^p\left(\rho_w^p\right)$ ($\mathrm{m}^2/(\mathrm{Vs})$) is the ion mobility parameter for ion type i in the pore system. The valence number for ion type i (to be used with the correct sign) is denoted by v_i $(-)$, and φ (V) denotes the electrical potential in the pore solution.

The mass exchange rate for the ion type i with solid constituents can, in a somewhat general case, be described as functions of all $\Re$ number of mol density concentrations of the different types of ions in phase p and all $\aleph$ number of mass densities of solid components in phase c. The mol density gain of mass to the i:th ion constituent dissolved in a pore solution from the solid phase is written as

$$\hat{n}_i^p = f_i\left(n_{i=1,...\Re}^p, \rho_{h=1,...\Im}^c\right) \tag{72}$$

And the mol density gain of mass to the h:th constituent in solid phase from ions in the pore solution is written as

$$\hat{n}_h = f_h\left(n_{i=1,...\Re}^p, \rho_{h=1,...\Im}^c\right) \tag{73}$$

where it should be noted that the function f_i is related to f_h through the chemical reaction assumed to be taking place.

The assumption for the electric displacement field d^p in a pore solution is

$$d^p = -\tilde{\varepsilon}\varepsilon_o \frac{\partial \varphi}{\partial x} \tag{74}$$

where ε_o (C/V) is the coefficient of dielectricity or permittivity of vacuum, $\varepsilon_o = 8.854 \cdot 10^{-12}$, and $\tilde{\varepsilon}$ (-) is the relative coefficient of dielectricity that varies among different dielectrics. For water at 25°C, $\tilde{\varepsilon} = 78.54$.

The charge density in a pore solution is the global unbalance of charge in a material point given as

$$q^p = F \sum_{i=1}^{\Re} n_i^p v_i \tag{75}$$

where $F = 96490$ (C/mol) is a physical constant describing the charge of one mol of an ion having a valence number equal to one.

Combining the mass balance (41) and constitutive relation (70) for the mass density flow of the water phase, one obtains

$$\frac{\partial \rho_w^p}{\partial t} = D_w^p \left(\breve{\rho}_w^p\right) \frac{\partial^2 \rho_w}{\partial x^2} \tag{76}$$

which is the governing equation determining $\rho_w^p(x,t)$.

Combining the constitutive relation (71), for the diffusion velocity for the ion type i, and the assumption (70) with the mass balance equation (65) for the same ion type, one obtains

$$\begin{aligned} \frac{\partial n_i^p}{\partial t} = {} & \tilde{D}_i^p \left(\breve{\rho}_w\right) \frac{\partial^2 n_i^p}{\partial x^2} + \tilde{A}_i^p \left(\breve{\rho}_w\right) v_i n_i^p \frac{\partial^2 \varphi}{\partial x^2} + \tilde{A}_i^p \left(\breve{\rho}_w\right) v_i \frac{\partial n_i^p}{\partial x} \frac{\partial \varphi}{\partial x} + \\ & \frac{D_w^p \left(\breve{\rho}_w\right)}{\rho_w} \frac{\partial \rho_w}{\partial x} \frac{\partial n_i^p}{\partial x} - \frac{n_i^p D_w^p \left(\breve{\rho}_w\right)}{\rho_w^2} \left(\frac{\partial \rho_w}{\partial x}\right)^2 + \\ & \frac{n_i^p D_w^p \left(\breve{\rho}_w\right)}{\rho_w} \frac{\partial^2 \rho_w}{\partial x^2} + f_i \left(n_{i=1,\ldots\Re}^p, \rho_{=1,\ldots\Im}\right) \end{aligned} \tag{77}$$

for all $i = 1, ..., \Re$ ion types considered.

The equation determining the mass density field $\rho_h^c(x,t)$ is obtained by combining the mass balance equation (40) and the constitutive assumption (73), i.e.

$$\frac{\partial \rho_h^c}{\partial t} = \xi_h \left(n_{i=1,\ldots\Re}^p, \rho_{h=1,\ldots\Im}\right); \qquad h = 1, ..., \aleph \tag{78}$$

where the function ξ_h is related to f_h, in (73), by the mol weight involved in the reaction. Explicit expressions describing mass exchanges between ions in a pore solution and the solid hydration products are proposed by constitutive equations in reports I:1-3. Examples of such reactions are binding of chlorides and leaching of hydroxide.

The governing equation for the electric potential $\varphi(x,t)$ is obtained by inserting the two constitutive assumptions (74) and (75) into the continuity equation (44), i.e.

$$-\tilde{\varepsilon}\varepsilon_o \frac{\partial^2 \varphi}{\partial x^2} = F \sum_{a=1}^{\Re} n_a v_a \tag{79}$$

According to the mass balance principle for the local mass exchanges between pore solution phase and solid phase, i.e. (43), the following should also hold

$$\sum_{i=1}^{\Re} f_i \left(n^p_{i=1,...\Re}, \rho^c_{h=1,...\Im} \right) = \sum_{b=1}^{\Im} f_h \left(n^p_{i=1,...\Re}, \rho^c_{h=1,...\Im} \right) \tag{80}$$

One of the main ideas behind this method of treating multicomponent ion diffusion in concrete pore solutions is that the diffusion parameters $\tilde{D}^p_i(\rho_w)$ and ion mobility parameters $\tilde{A}^p_i$ for all i:th types of ions considered can be scaled with the same tortuosity factor t, which is assumed to be a function of the moisture content ρ_w. That is

$$\tilde{D}^p_i = t(\rho_w) D_i; \qquad \tilde{A}^p_i = t(\rho_w) A_i; \qquad i = 1, ..., \Re$$

where D_i and A_i are the bulk diffusion and ion mobility coefficient in water, respectively. The values of these coefficients for different types of ions can be found in, for example, [10]. The experimental work concerning the diffusion characteristics, therefore, consists of determining only one parameter, i.e. $t(\rho_w)$ for the material in question. The main experimental and theoretical work, due to this choice of approach, is directed more towards describing the mass exchanges between ions in pore solution and the solid components of concrete, i.e. the description of f_i and f_h.

In reports I:1-3 the parameter $t(\rho_w)$ is evaluated at saturated conditions for different concrete qualities. In these papers different mass exchange assumptions are also included.

In paper 2 the convective driven diffusion due to capillary suction and normal diffusion of chlorides is examined. A more simplified version of the

governing equations than those derived in this section is used; the main concept is, however, the same.

The numerical problems associated with the present convective term in the $\Re$ number of equations shown in (77) are analyzed, for the typical length and time scales in the problem studied, in paper 3.

3.3.3 Methods of measurements of chloride penetration into hardened concrete

Different methods determining the diffusion characteristics of chlorides in the pore system of concrete are discussed in this section. It is noted, however, that it is difficult to perform measurements on the separate mechanisms listed in section 3.3.1. The measured response must rather be seen as a combined effect of many different phenomena.

Colorimetric method: One of the first methods adopted to indicate the depth of penetration of external chlorides into concrete was a simple colorimetric method, e.g. see . It is based on the spraying of fluorescein (1g/l in a 70% of ethyl alcohol in water) and then of silver nitrate aqueous solution (0.1 M $AgNO_3$) on the concrete fractured surface area. In the absence of chlorides, or in the presence of chemically bound chlorides only, the concrete surface becomes dark when exposed to natural light. In the presence of free chlorides in a pore solution of concrete, AgCl is formed which produces a pink color in the presence of fluorescein.

The method cannot directly be used to identify material constants related to the chloride ion diffusion. The method is, however, ideally suited for rapid testing of the condition of concrete structures.

Ion selective electrodes: Samples from concrete are collected by drilling or grinding. The powder is normally stored in a liquid based on a nitric acid which dissolves both free and bound chlorides. A chloride sensitive electrode is calibrated against several different solutions with known concentrations of chloride. The calibrated electrode measures the voltage for the sample solution. The reading is converted to a chloride concentration given by the calibration procedure. The chloride concentration is often given as mass chlorides by concrete mass.

The method described has been used to detect chlorides in the experiments described in reports I:1-3.

Potentiometric titration: This equipment measures chloride ion concentrations in the interval 10-999 mg Cl^-/l. The repeatability is about $\pm 1.5\%$ at an absolute level of 200 mg Cl^-/l. The calibration is performed on a 500 μl sample at the concentration 200 mg Cl^-/l. A potentiometer is adjusted until the correct reading is obtained.

During the experiment the chloride solution to be tested is in contact with two electrodes. Silver ions are supplied from the silver anode by applying a constant current. When all chloride ions have been consumed by the silver ions, the same ions increase rapidly in solution and a 'dead stop' function stops the current. The time period for having the constant current applied to the solution serves as a measure of the number of dissolved chloride ions in the test.

Potentiometric titration has been used as a complementary method to the ion selective electrode, see reports I:1-3.

X-ray mapping: A scanning electrode microscope has been used to detect chlorides in cement paste [7]. Samples were exposed to a 3% NaCl solution for three hours. The samples were dried in a direction perdenticular to the one dimensional chloride diffusion direction. This was done to minimize further penetration of chlorides within the paste. The X-ray mapping of the chloride penetrated samples indicated a depth of penetration. However, the concentrations of chlorides in the sample in this experiment were so low that the general noise in the signals effectively shaded the exact chloride profile and hence the exact penetration depths. The method can probably be improved for samples exposed to higher chloride ion concentrations. Further developments of the method are of interest since several types of ions can be detected with the X-ray analysis, which means that the effect of the composition of the pore solution and the outer storage solution can be studied.

Steady state diffusion cell tests: A concrete disc is placed between two compartments containing solutions at different concentrations of chlorides, e.g. see [12]. The solutions in the two compartments are often saturated with $Ca(OH)_2$ to minimize leaching from the sample. Typically a 1 M NaCl solution in saturated $Ca(OH)_2$ is used in the up-stream compartment and a saturated $Ca(OH)_2$ solution in the down-stream compartment. The concentrations of chloride ion in the down-stream compartment after various diffusion times can be determined by withdrawing small volumes of the so-

The governing equation becomes

$$\frac{\partial \rho_c}{\partial t} = D_{ct}\frac{\partial^2 \rho_c}{\partial x^2} + A_{ct}\rho_c\frac{\partial^2 \phi}{\partial x^2} + A_{ct}\frac{\partial \rho_c}{\partial x}\frac{\partial \phi}{\partial x} \tag{86}$$

where (84) and (85) are used.

The experiment can be controlled so that $\partial\phi/\partial x = const. = E$, i.e. $\partial^2\phi/\partial x^2 = 0$, which means that the equation (86) can be written

$$\frac{\partial \rho_c}{\partial t} = D_{ct}\frac{\partial^2 \rho_c}{\partial x^2} + \frac{D_{ct}zFE}{RT}\frac{\partial \rho_c}{\partial x} \tag{87}$$

where the relation $A_{ct} = D_{ct}zF/(RT)$ is used.

If using a sufficient high applied electrical field, i.e. $EzF/(RT) >> 1$, it can be motivated to set the pure diffusion term $D_{ct}\partial^2\rho_c/\partial x^2 = 0$. For the initial conditions and applied boundary conditions used in terms of chloride concentration and the electrical potential, the sharp penetration front is, in this case, simply given as

$$x_f = tD_{ct}zFE/(RT) \tag{88}$$

which is the condition obtained from (87) when the applied electrical field is sufficiently high. That is, the expression (87) is the integrated version of the equation $x_c^{'} = D_{ct}zFE/(RT)$ which is valid from the given assumptions together with equation (85). The term $D_{ct}zFE/(RT)$ corresponds to the 'drift' velocity of the chlorides due to the constant electrical 'force' when the pure diffusion, caused by concentration gradients, can be neglected.

By measuring the penetration depth with the colorimetric method which during ideal conditions is the x_f-value, the diffusion constant D_{ct} can be calculated for a given exposure duration t, using equation (88).

It can be argued that some improvements of the model on which the experiments are evaluated can be made. The strategy is to solve equation (87) analytically with proper boundary conditions in which the D_{ct}-value obtained from equation (88) is used. The penetration depth of chlorides from this calculation is compared with the calculated values given from expression (88), see Figure 1.

For the range of electrical fields E adopted in the experiments, the following relation between the ideal penetration depth x_f and the penetration depth obtained from solving equation (87) has been proposed [13]:

$$x_f = x_d + x_d^r \tag{89}$$

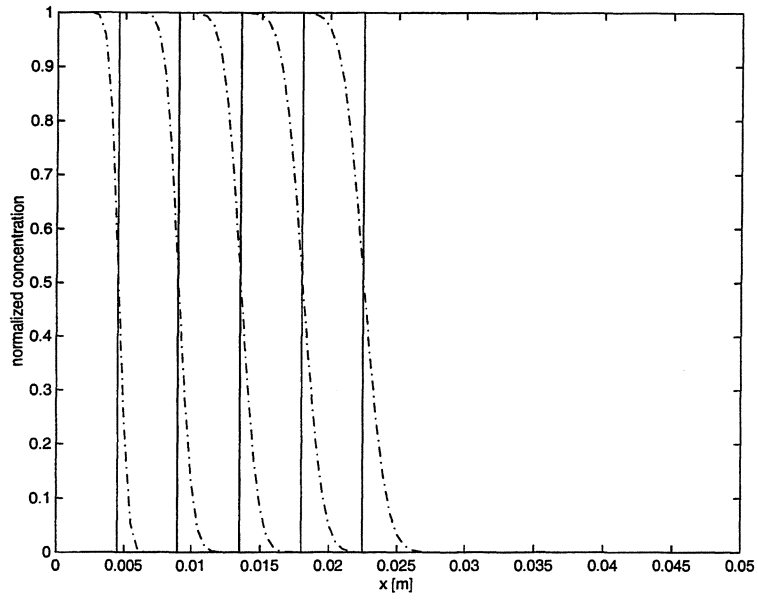

Figure 1: *Schematic illustration of the solutions of equation (21), solid line, and equation (20), dashed line, for given values of the diffusion constant and the applied electrical field E. A normalized boundary condition has been used.*

where the r is a parameter approximately equal to 0.5. If the colorimetric method is very sensitive for low concentrations of chlorides, the x_d value can be used as the measured penetration depth instead of x_f. In this case (89) and (88) should be used to calculate D_{ct}.

The robustness of the method can be checked in a number of ways. As an example, the D_{ct}-values can be calculated from the experiment at different exposure times. Obtained differences of these values then serve as a measure of the error in the evaluation technique. Another approach is to measure the chloride ion profile, after a given exposure duration in the migration cell, which according to the adopted evaluation method should be identical to the profile given from solving equation (87) with properly applied boundary conditions.

Total chloride profile tests: Samples from concrete are removed from certain distances from the surface previously exposed to a chloride solution with constant concentration at entire exposed surface (immersed condition).

The sampling can be performed by using a more sophisticated grinding device or simply by drilling. The collected concrete powder is analyzed by an ion selective electrode or by potentiometric titration as described previously.

The method behind the total chloride profile test is to match the measured chloride concentration profile to the solution of a modified Fick's second law, e.g. see [14]. The method incorporates binding of chlorides only during special conditions which will be explained in the following.

Consider first the mass balance equation for the 'free' chlorides in a pore solution including also mass exchange with the solid hydration products in concrete, i.e.

$$\frac{\partial \rho_{cf}}{\partial t} = -\frac{\partial}{\partial x}\left(\rho_{cf} x'_{cf}\right) + \hat{r}_{cf} \tag{90}$$

where ρ_{cf} is the mass concentration density of chlorides, x'_{cf} is the velocity of free chlorides and $\hat{r}_{cf}$ is the gain of free chlorides from the bound chlorides.

The mass balance equation for the chemically or physically bound chlorides is

$$\frac{\partial \rho_{cb}}{\partial t} = -\frac{\partial}{\partial x}\left(\rho_{cb} x'_{cb}\right) + \hat{r}_{cb} \tag{91}$$

where ρ_{cb} is the mass concentration density of bound chlorides, x'_{cf} is the velocity of bound chlorides and $\hat{r}_{cf}$ is the gain of bound chlorides from the free chlorides in pore solution.

The last mass balance principle is the conservation of mass for the considered mass exchange between free and bound chlorides, i.e.

$$\hat{r}_{cf} = -\hat{r}_{cb} \tag{92}$$

The constitutive equation for the mass density flow of free chlorides is

$$\rho_{cf} x'_{cf} = -D_c \frac{\partial \rho_{cf}}{\partial x} \tag{93}$$

where D_c is the diffusion constant for chloride ions in pore solution.

The mass density flow of bound chlorides is set to zero i.e.

$$\rho_{cb} x'_{cb} = 0 \tag{94}$$

A quasi-static condition is assumed for the mass exchange of free and bound chlorides. It is assumed that an equilibrium between free and bound chlorides is always satisfied, as

$$\rho_{cb} = K \rho_{cf} \tag{95}$$

where K is a constant, representing the slope of the so-called chloride binding isotherm assuming this to be linear. The validity of this assumption has been questioned, for example, in [13] and [15]. The assumption (95) also states that the equilibrium condition between ρ_{cb} and ρ_{cf} is reached instantaneously during all conditions. Combining equations (90)-(95) results in the equation

$$\frac{\partial \rho_{cf}}{\partial t} = \frac{D_c}{(1+K)} \left(\frac{\partial^2 \rho_{cf}}{\partial x^2} \right) \tag{96}$$

where the constant term $D_c/(1+K)$ can be referred to as a special type of diffusion constant incorporating linear binding; this constant will be denoted D_c^*, i.e.

$$D_c^* = \frac{D_c}{(1+K)} \tag{97}$$

Hence, the equation for the free diffusing ions subjected to linear binding can be written as

$$\frac{\partial \rho_{cf}}{\partial t} = D_c^* \left(\frac{\partial^2 \rho_{cf}}{\partial x^2} \right) \tag{98}$$

The measurement of chloride profiles is almost always the total chloride concentration, i.e. $\rho_{ct}(x) = \rho_{cb}(x) + \rho_{cf}(x)$. According to the assumed conditions the ratio between the mass density concentration of free chloride and total chloride should be constant for all penetration depths studied, i.e.

$$\frac{\rho_{cf}(x)}{\rho_{cb}(x) + \rho_{cf}(x)} = \frac{1}{K+1} = \text{const.} \tag{99}$$

where (95) is used.

The value K can be predicted from the experiment by using the measured mass density concentration of total chloride near $x = 0$, i.e. at the exposed surface. The free mass density concentration in pore solution at $x = 0$ is assumed equal to the storage solution. From (99) the linear binding capacity K is calculated as $K = \rho_{ct}(0)/\rho_{cf}(0) - 1$, where $\rho_{ct}(0) = \rho_{cb}(0) + \rho_{cf}(0)$ is the measured total mass density concentration of chlorides just beneath the exposed concrete surface. The value $\rho_{cf}(0)$ is the boundary condition, i.e. the concentration in outer storage solution.

The value K obtained from the above analysis is used to scale the measured total mass density concentration at all spatial locations in the one-dimensional domain: as $\rho_{cf}(x) = \rho_{ct}(x)/(K+1)$. The obtained free chloride profile $\rho_{cf}(x)$ is used together with the equation (98). Test values of

D_c^* are tried out until a satisfactory match between the free chloride profile $\rho_{cf}(x)$, obtained from the experiments for a given exposure time, and the calculated profiles are obtained. From the best fitted diffusion constant D_c^* and from the value of K , the diffusion constant for free chlorides in pore system D_c can be calculated by the equation (97). If all methods discussed for determining the free diffusion constant of chlorides in a pore system of concrete are significant, the obtained D_c, from the total chloride profile test, should not differ from values obtained by any of the above discussed diffusion cell methods.

It is often observed in experiments that the maximum chloride content is a few millimeters from the exposed surface even when using a constant outer concentration of chlorides. During such a condition the above described approach, calculating the D_c^* D_c and K value, should not be used since the basic assumptions involved in evaluating these properties, in this case, are in conflict with the experimentally obtained observations.

It should be observed that the so-called effective diffusion constant, denoted D_c^{eff}, is the diffusion constant obtained by fitting equation (98) to the total chloride profile without any special attention to the real applied boundary condition in the experiment.

The correctness of the model leading to D_c^* D_c and K can be tested by, for example, using different storage concentrations and exposure times. The material constants obtained for such tests should be independent of different constant storage conditions and exposure times. Another way of checking the significance of the obtained constants, describing the chloride diffusion characteristics, is to compare the free diffusion constant D_c with corresponding constants obtained from other techniques.

A method similar to the one described in this section has been adopted as a part of the investigations performed in reports I:1-3.

Pore expression method: Above it was concluded that the binding capacities can be estimated from the total chloride profile test by measuring the total chloride content at the exposed surface for different outer mass density concentrations of chloride. The method assumes that the free chloride concentration in pore solution near the exposed surface in concrete is the same as the outer solution. Here a method will be described in which the concentration of chlorides, or/and the concentration of other types of ions, in a pore solution are measured in an explicit manner.

The method is based on expressing the pore solution by applying an external pressure to the sample, e.g. see [16]. The drained solution is collected and analyzed for different types of ions using standard techniques, such as titration. The use of the pore press method is well established, and much data has been acquired in this manner. It is noted, however, that the technique overestimates the free chloride levels. This is presumably caused because loosely bound chlorides are affected by the applied pressure. The use of the pore press also presents difficulties when applied to concrete specimens with the presence of coarse aggregate particles. The method cannot be used on concrete with very low water to binder ratio because the amount of pore liquid accessible to chloride (the capillary pores) is to low.

Gas diffusion technique, an indirect method: The diffusion constant for chlorides or other types of ions in concrete can be predicted by a gas diffusion technique [17]. The apparatus consists of two diffusion cells separated by a thin dry concrete disc. One of the cells contains nitrogen gas and the other helium. The change of the concentration of nitrogen molecules in a cell is measured with respect to a reference cell, located outside the diffusion cell, containing a constant concentration of helium gas. Thermistors are affixed to the diffusion and reference cells which measure the change of thermal conductivity of the gas phase as it varies with time. The counter diffusion of the helium and nitrogen measured through the concrete is used to establish a porosity-to-tortuosity factor. The effective chloride ion diffusion in concrete is a function of the porosity-to-tortuosity factor and the diffusion coefficient of chloride ions in bulk water, which is a known value. Excellent results has been obtained with this method when correlated with the conventional diffusion measurement techniques for concretes having different water to cement ratios and cement contents.

3.4 Moisture transport

3.4.1 A steady-state isothermal method for measuring the moisture transport coefficient as a function of moisture content

The two most important properties affecting ion transport, which is related to the moisture condition in concrete, are the concentration of liquid water in the pore space and the capillary suction velocity of the water phase. That is, a somewhat general description of diffusion of different types of ions in a pore solution needs the information of the flow characteristics and mass density concentration of water in the pore system. A direct and simple way of measuring the material function $D_w(\rho_w)$ which yields the desired properties, when used in Fick's second law, will be presented in this section. The experimental methods described in sections 3.4.1 and 3.4.2 can be used. The technique to be presented, evaluating $D_w(\rho_w)$ at steady state conditions, is described in [18]. Applications on different cement based building materials can be found in [19].

The assumption for the mass density flow $\rho_w x_w'$ (kg/(m^{2}s)) is the non-linear assumption

$$\rho_w x_w' = -D_w(\rho_w)\frac{\partial \rho_w}{\partial x} \tag{100}$$

The mass balance equation without any mass exchanges in one dimension is

$$\frac{\partial \rho_w}{\partial t} = -\frac{\partial}{\partial x}\left(\rho_c x_c'\right) \tag{101}$$

Combining the constitutive equation (100) and the mass balance equation (101) gives

$$\frac{\partial \rho_w}{\partial t} = \frac{\partial}{\partial x}\left(D_w(\rho_w)\frac{\partial \rho_w}{\partial x}\right) \tag{102}$$

The mass density flow $\rho_w x_w'$ can be described with other state variables than ρ_w. Consider a new potential denoted χ being related to ρ_w with a function $\rho_w = f(\chi)$. If we identify χ as the relative humidity, the function $\rho_w = f(\chi)$ is the sorption isotherm. The flow $\rho_w x_w'$ can be described by the potentials ρ_w, χ or ψ, as

$$\rho_w x_w' = -D_w(\rho_w)\frac{\partial \rho_w}{\partial x} = -D_\chi(\chi)\frac{\partial \chi}{\partial x} = -\frac{\partial \psi}{\partial x} \tag{103}$$

It is directly noted that the diffusion parameters $D_w(\rho_w)$ and $D_\chi(\chi)$ are related as

$$\frac{D_\chi(\chi)}{D_w(\rho_w)} = \frac{\partial \rho_w}{\partial \chi} \tag{104}$$

That is, with χ being the relative humidity the ratio $D_\chi(\chi)/D_w(\rho_w)$ is the slope of the sorption isotherm. The variable ψ, referred to as the Kirchhoff potential, is a function corresponding to a case where the diffusion constant becomes identical to unity. According to the relations in (103) ψ is related to $D_\chi(\chi)$ and $D_w(\rho_w)$ as

$$d\psi = D_\chi(\chi)\, d\chi; \quad \text{and} \quad d\psi = D_w(\rho_w)\, d\rho_w \tag{105}$$

Hence, ψ can be identified as

$$\psi = \int_{\chi_{ref}}^{\chi} D_\chi(\chi)\, d\chi \tag{106}$$

Combining the mass balance equation (101) with the constitutive relation (103) expressed with the gradient of the Kirchhoff potential ψ, one obtains

$$\frac{\partial \rho_w}{\partial t} = \frac{\partial}{\partial x}\left(\frac{\partial \psi}{\partial x}\right) \tag{107}$$

The chain rule can be used to express the time derivative of ρ_w in terms of the potential ψ, as

$$\frac{\partial \rho_w}{\partial t} = \frac{\partial \rho_w \partial \psi}{\partial \psi \partial t} = C_\psi(\psi)\frac{\partial \psi}{\partial t} \tag{108}$$

Combining (107) and (108) gives the governed equation corresponding to (102), now being expressed in terms of the potential ψ, i.e.

$$\frac{\partial \psi}{\partial t} = \frac{1}{C_\psi(\psi)}\frac{\partial}{\partial x}\left(\frac{\partial \psi}{\partial x}\right); \quad \psi = f_\psi(\chi); \quad C_\psi = \frac{\partial \rho_w}{\partial \psi}; \quad \rho_w = f_\chi(\chi) \tag{109}$$

A stationary condition will be defined in which $\partial \rho_w / dt = 0$. From this condition it follows that

$$\frac{\partial}{\partial x}\left(\frac{\partial \psi}{\partial x}\right) = 0; \quad \frac{\partial \psi}{\partial x} = const. = -\rho_w x_w'; \tag{110}$$

where (107) is used. Integration of $\partial \psi / \partial x = -\rho_w x_w'$ gives

$$\psi = \left(\rho_w x_w'\right) x + \psi_o \tag{111}$$

This relation can be used when evaluating experiments in two ways. Consider first the cup method (stationary flow) in which the mass density flow, i.e. the gradient of ψ, through a specimen with thickness L is measured. The condition at $x = 0$ is $\psi_o = 0$ with the relative humidity χ_o, and at $x = L$ different χ_i are used. For each applied χ_i the mass density flow $\left(\rho_w x_w'\right)_i$ is measured. Hence, using the cup-method the discrete function $\psi_i = \psi_i(\chi_i)$ is measured using the relation (111), i.e.

$$\psi_i = \left(\rho_w x_w'\right)_i L; \qquad \chi = \chi_i; \qquad (\longrightarrow \psi_i = \psi_i(\chi_i)); \qquad 0 \leq x_i \leq L \quad (112)$$

where χ_i are the different tested relative humidities at $x = L$.

In order to solve the governed equation (111), not only $\psi = f_\psi(\chi)$ must be known but also $C_\psi = \partial\rho_w/\partial\psi$, which is determined from the measured sorption isotherm, i.e. the measured function $\rho_w = f_\chi(\chi)$.

Another nice property of the Kirchhoff potential is that the diffusion parameter $D_w(\rho_w)$ can be obtained from measurements on one-dimensional steady state moisture profiles and also by measuring the corresponding constant mass density flow passing through the sample. At $x = 0$ the experimental condition is $\psi_o = 0$ and χ_o, and at $x = L$ a constant relative humidity different from χ_o are used. The measured relative humidity profiles and measured mass flow at equilibrium determine the discrete function $\psi_i = \psi_i(\chi_i)$ using (111), i.e.

$$\psi_i = \left(\rho_w x_w'\right) x_i; \qquad \chi = \chi_i; \qquad (\longrightarrow \psi_i = \psi_i(\chi_i)); \qquad 0 \leq x_i \leq L \quad (113)$$

where the χ_i values are the relative humidities at the different depths x_i.

The governing equation (109) can be used for solving one-dimensional transient moisture transport problems in porous materials when the functions $\psi = f_\psi(\chi)$, $C_\psi = \partial\rho_w/\partial\psi$ and $\rho_w = f_\chi(\chi)$ have been evaluated. The numerical solution procedure actually becomes simplified as compared to the solution of (102) since the function C_ψ is less nonlinear than the function D_w.

The concept behind the Kirchhoff potential is used in paper 2 dealing with combined moisture and chloride ion flow in concrete.

The method is not developed for the use at moisture levels above the hygroscopic range (i.e. above about 98% relative humidity). The method described in section 3.4.2. is, however, suited for evaluating the moisture transport coefficient at very high moisture levels.

3.4.2 Calculation of the moisture transport coefficient as a function of moisture content from a series of capillary suction experiments

If the mass gain during a one-dimensional, semi-infinite, capillary suction experiment performed on a porous material is shown to be proportional to the square root of exposure time for different initial moisture contents, the material function $D_w(\rho_w)$, as used in Fick's second law, can be calculated in an explicit manner. The reason for this is that the time derivative of the total uptake of water due to capillary suction can be interpreted as a boundary condition related to the square root of exposure time; this square root dependence is also present in Fick's first law describing the flow characteristics within material when using a so-called Boltzmann transformation. It turns out that the square root dependence cancels when using the Boltzmann variable, i.e. $\eta = x/\left(2\sqrt{t}\right)$, which means that a piece-wise linear function, relating the mass density flow of water to the gradient of the mass density concentration of water, can be calculated. The approach is described in [18] and experimental verifications can be found in [20].

The first assumption is that the determination of the mass density concentration of liquid water $\rho_w(x,t)$ in the material can be given by Fick's second law, i.e.

$$\frac{\partial \rho_w}{\partial t} = \frac{\partial}{\partial x}\left(D_w(\rho_w)\frac{\partial \rho_w}{\partial x}\right) \tag{114}$$

Consider a semi-infinite one-dimensional case where a material is gaining water in the domain

$$W_n(t) = \int_0^\infty (\rho_w(x,t) - \rho_{wn})\,dx \tag{115}$$

where $W_n(t)$ (kg/m^2) is the total gain of water passing through the exposed surface within a given area. The capillary constant A_n (kg/(m^{2}s$^{1/2}$)) for a test when the initial mass density concentration of water in the material is ρ_{wn}, is related to $W_n(t)$, as

$$W_n(t) = A_n\sqrt{t}; \quad \text{with} \quad \rho_{wn} \tag{116}$$

where it should be noted that far from all porous materials fulfill this relation during capillary suction. Furthermore, it is important to observe that the capillary sucked water is not allowed to be affected by the opposite side of

that being exposed to water, i.e. the semi-infinite geometrical assumption must be valid during all time levels.

The function $\rho_w(x,t)$ in equation (114) is described with a function f as:

$$\rho_w(x,t) = f(n); \qquad \eta = \frac{x}{2\sqrt{t}} \tag{117}$$

which is the so-called Boltzmann transformation.

The initial conditions for the considered semi-infinite condition are

$$\rho_w(x,0) = \rho_{wn}; \qquad x > 0; \quad \rightarrow \quad f(\infty) = \rho_{wn} \tag{118}$$

The boundary condition at $x = 0$ is

$$\rho_w(0,t) = \rho_{wcap}; \qquad t > 0; \quad \rightarrow \quad f(0) = \rho_{wcap} \tag{119}$$

where ρ_{wcap} is the capillary saturation.

The needed time derivative in (114) expressed in terms of the variable η, in equation (117), becomes

$$\frac{\partial \rho_w}{\partial t} = \frac{\partial f}{\partial \eta}\frac{\partial \eta}{\partial t} = \frac{\partial f}{\partial \eta}\eta\left(-\frac{1}{2t}\right) \tag{120}$$

and the spatial derivative $\partial^2\rho_w/\partial x^2$, described in terms of η, is obtained by noting that

$$\frac{\partial \rho_w}{\partial x} = \frac{\partial f}{\partial \eta}\frac{\partial \eta}{\partial x} = \frac{\partial f}{\partial \eta}\left(-\frac{1}{2\sqrt{t}}\right) \tag{121}$$

i.e.

$$\frac{\partial^2 \rho_w}{\partial x^2} = \frac{\partial^2 f}{\partial \eta^2}\left(\frac{1}{4t}\right) \tag{122}$$

Combining (114) with (120) and (121) yields

$$\frac{\partial^2 f}{\partial \eta^2} + \left(\frac{2\eta}{D_w(f(\eta))}\right)\frac{\partial f}{\partial \eta} = 0 \tag{123}$$

which is Fick's second law expressed in terms of the new variable η.

The boundary condition at $x = 0$ will be described with a mass density flow, i.e.

$$\left(\rho_w x_w'\right)_{x=0} = -D_w(\rho_w)\left(\frac{\partial \rho_w}{\partial x}\right)_{x=0} = -D_w(f(\eta))\left(\frac{\partial f}{\partial \eta}\left(-\frac{1}{2\sqrt{t}}\right)\right)_{\eta=0} \tag{124}$$

The flow of water through the surface at $x = 0$ is identical to the time derivative of the measured function W_n. This condition expressed in terms of the variable η is

$$\frac{\partial W_n}{\partial t} = \frac{A_n}{2\sqrt{t}} = -D_w\left(f\left(\eta\right)\right)\left(\frac{\partial f}{\partial \eta}\left(-\frac{1}{2\sqrt{t}}\right)\right)_{\eta=0} \tag{125}$$

where (116) and (124) are used. That is, the capillary number A_n is related to the material function $D_w\left(f\left(\eta\right)\right)$, as

$$A_n = -D_w\left(f\left(\eta\right)\right)\left(\frac{\partial f}{\partial \eta}\right)_{\eta=0} \tag{126}$$

The integration of (123) can be performed by noting that

$$\frac{\frac{\partial^2 f}{\partial \eta^2}}{\frac{\partial f}{\partial \eta}} = \frac{\partial}{\partial n}\left(\ln\left|\frac{\partial f}{\partial \eta}\right|\right) = -\frac{2\eta}{D_w\left(f\left(\eta\right)\right)} \tag{127}$$

Integration of (127) from 0 to η, using s as an integration variable, yields

$$\ln\left|\frac{\partial f\left(\eta\right)}{\partial \eta}\right| - \ln\left|\frac{\partial f\left(0\right)}{\partial \eta}\right| = -\int_0^{\eta} \frac{2s}{D_w\left(f\left(s\right)\right)} ds \tag{128}$$

i.e. the derivative $\partial f\left(\eta\right)/\partial \eta$ can be expressed as

$$\frac{\partial f\left(\eta\right)}{\partial \eta} = \left(\frac{\partial f}{\partial \eta}\right)_{\eta=0} \exp\left(-\int_0^{\eta} \frac{2s}{D_w\left(f\left(s\right)\right)} ds\right) \tag{129}$$

Combining (126) and (129) gives

$$\frac{\partial f}{\partial \eta} = -\frac{A_n}{D_w\left(f\left(\eta\right)\right)} \exp\left(-\int_0^{\eta} \frac{2s}{D_w\left(f\left(s\right)\right)} ds\right) \tag{130}$$

Yet another integration of (130) gives

$$f\left(\eta\right) - f\left(0\right) = -\frac{A_n}{D_w\left(f\left(\eta\right)\right)} \int_0^{\eta} \left\{\exp\left(-\int_0^{s'} \frac{2s}{D_w\left(f\left(s\right)\right)} ds\right)\right\} ds' \tag{131}$$

which involves the step response given by $f\left(\eta = \infty\right) = \rho_{wn}$ and $f\left(0\right) = \rho_{wcap}$ and the unknown value of $D_w\left(f\left(\eta\right)\right)$ corresponding to the measured property

A_n. From (118), (119) and (131) it is concluded that

$$\begin{aligned} f(0) - f(\infty) &= \rho_{wcap} - \rho_{wn} \\ &= \frac{A_n}{D_w(f(n))} \int_0^\infty \left\{ \exp\left(- \int_0^{n'} \frac{2s}{D_w(f(s))} ds \right) \right\} ds' \end{aligned} \tag{132}$$

The equation (130) gives

$$\frac{\partial f}{\partial \eta} = - \frac{A_n}{D_w(f(\eta))} \exp\left(- \frac{\eta^2}{D_w(f(\eta))} \right) \tag{133}$$

The experimental procedure is to conditioning samples at different initial mass density concentrations of water

$$\rho_{winitial} = \rho_{w1}, \rho_{w2}, \ldots \rho_{wN}; \qquad \rho_{wcap} > \rho_{w1} > \rho_{w2} > \ldots > \rho_{wN} \tag{134}$$

where ρ_{wcap} is the capillary saturation. Piece-wise constant values of the material function $D_w(\rho_w)$ are searched for in the N number of intervals, according to

$$D_w(\rho_w) = \left\{ \begin{array}{cc} D_1 & \rho_{wcap} > \rho_w > \rho_{w1} \\ D_2 & \rho_{w1} > \rho_w > \rho_{w2} \\ & \vdots \\ D_N & \rho_{wN-1} > \rho_w > \rho_{wN} \end{array} \right\} \tag{135}$$

The corresponding N capillary numbers should be evaluated at the following conditions

$$A_n(\rho_{winitial}) = \left\{ \begin{array}{cc} A_1 & \rho_{winitial} = \rho_{w1} \\ A_2 & \rho_{winitial} = \rho_{w2} \\ & \vdots \\ A_N & \rho_{winitial} = \rho_{wN} \end{array} \right\} \tag{136}$$

The condition in (132) determines the piece wise constant property D_1 for $n = 1$, for the tested step response, i.e.

$$\begin{aligned} \rho_{wcap} - \rho_{w1} &= \frac{A_1}{D_1} \int_0^\infty \exp\left(- \frac{\eta^2}{D_1} \right) d\eta \\ &= \left[\eta = s\sqrt{D_1} \right] \\ &= \frac{A_1 \sqrt{D_1}}{D_1} \int_0^\infty \exp\left(-s^2 \right) ds \end{aligned} \tag{137}$$

The integral $\int_0^\infty \exp(-s^2)\,ds$ in equation (137) is equal to $\sqrt{\pi}/2$, therefore A_1 and D_1 are related as

$$\rho_{wcap} - \rho_{w1} = \frac{A_1\sqrt{\pi}}{2\sqrt{D_1}} \tag{138}$$

when the initial moisture condition in the test is ρ_{w1} and the capillary saturation is ρ_{wcap}. The equation (138) is used to solve the constant diffusion value D_1 in the interval $\rho_{wcap} > \rho_w > \rho_{w1}$ which is derived from the experimental conditions from which also A_1 is measured.

Consider next two piece-wise linear diffusivities D_1 and D_2 with $\rho_{w2} = \rho_{winitial}$ and let η_1 be the η value in which the function f is ρ_{w1}, i.e.

$$f(\eta_1) = \rho_{w1} \tag{139}$$

In the interval $0 \leq \eta \leq \eta_1$, i.e. $\rho_{wcap} > \rho_w > \rho_{w1}$, the constant value D_1 is valid. In a test with the initial value ρ_{w2} the capillary number A_2 is measured. For this case equation (133), gives

$$\frac{\partial f}{\partial \eta} = -\frac{A_2}{D_1}\exp\left(-\frac{\eta^2}{D_1}\right) \tag{140}$$

Integration of (140) in the interval $0 \leq \eta \leq \eta_1$ results in

$$f(\eta_1) = \rho_{w1} = \rho_{wcap} - \frac{A_2}{D_1}\exp\left(-\int_0^{n_1}\frac{\eta^2}{D_1}d\eta\right) \tag{141}$$

Using the integration variable $\eta = s\sqrt{D_1}$ and noting that the exponential function can be expressed with the error function defined as $\mathrm{erf}(\xi) = \frac{2}{\sqrt{\pi}}\exp\left(\int_0^\xi\left(-\xi^2\right)d\xi\right)$, equation (141) can be written

$$\rho_{wcap} - \rho_{w1} = \frac{\sqrt{\pi}A_2}{2\sqrt{D_1}}\,\mathrm{erf}\left(\frac{\eta_1}{\sqrt{D_1}}\right) \tag{142}$$

It is noted that the experimental conditions ρ_{wcap} and ρ_{w1} together with the measured values of A_1 and A_2 give information of the property η_1 which is solved by combining (138) and (142).

The expression determining the constant value D_2 in the interval $\rho_{w1} > \rho_w > \rho_{w2}$ is obtained by using equation (133). Integration in the domain

$0 \leq \eta \leq \infty$ gives

$$\begin{aligned} \frac{\partial f}{\partial \eta} &= -\frac{A_2}{D_2} \exp\left(-\int_0^{n_1} \frac{2\eta}{D_1} d\eta - \int_{n_1}^{n} \frac{2\eta}{D_2} d\eta\right) \\ &= -\frac{A_2}{D_2} \exp\left(-\frac{\eta_1^2}{D_1} - \frac{1}{D_2}\left(\eta^2 - \eta_1^2\right)\right) \end{aligned} \tag{143}$$

Integrating (143) from η_1 to $\eta = \infty$ gives the equation determining the D_2 value in the interval $\rho_{w1} > \rho_w > \rho_{w2}$, i.e.

$$\begin{aligned} f(\eta) &= \rho_{w1} - \frac{A_2}{D_2} \exp\left(-\left(\frac{1}{D_1} - \frac{1}{D_2}\right)\eta_1^2\right) \int_{n_1}^{n} \frac{2\eta}{D_1} d\eta \\ &= \rho_{w1} - \frac{A_2\sqrt{\pi}}{2\sqrt{D_2}} \exp\left(-\left(\frac{1}{D_1} - \frac{1}{D_2}\right)\eta_1^2\right)\left(\operatorname{erf}\left(\frac{\eta}{\sqrt{D_2}}\right) - \operatorname{erf}\left(\frac{\eta_1}{\sqrt{D_2}}\right)\right) \end{aligned} \tag{144}$$

where $f(\eta = \infty) = \rho_{w2}$ and it is noted that

$$\operatorname{erf}\left(\frac{\eta}{\sqrt{D_2}}\right) = 1 \quad \text{when} \quad \eta = \infty \tag{145}$$

That is , the measured properties ρ_{wcap}, ρ_{w1}, ρ_{w2}, A_1 and A_2 give the unknown values D_1, D_2 and η_1 by the three equations

$$\rho_{wcap} - \rho_{w1} = \frac{A_1\sqrt{\pi}}{2\sqrt{D_1}} \tag{146}$$

$$\rho_{wcap} - \rho_{w1} = \frac{\sqrt{\pi}A_1}{2\sqrt{D_1}} \operatorname{erf}\left(\frac{\eta_{2,1}}{\sqrt{D_1}}\right) \tag{147}$$

$$\rho_{w1} - \rho_{w2} = \frac{A_2\sqrt{\pi}}{2\sqrt{D_2}} \exp\left(-\left(\frac{1}{D_1} - \frac{1}{D_2}\right)\eta_{2,1}^2\right)\left(1 - \operatorname{erf}\left(\frac{\eta_{2,1}}{\sqrt{D_2}}\right)\right) \tag{148}$$

where η_1 has been replaced by $\eta_{2,1}$ to stress that this value is only related to the case of two intervals.

Next consider the equations for determining N number of piece-wise constant D-values. The break points are then given as

$$f(\eta = 0) = \rho_{wcap} \text{ and } f(\eta_n) = \rho_{wn}; \qquad n = 1, ...N \tag{149}$$

The derivative $\partial f/\partial \eta$ can be described for each interval in the same manner as described above. The function $f(\eta)$ is established by integrations in the

correct domains corresponding to the intervals used in the experiments which determine the $A_{n=1,\ldots N}$ values. The N numbers of equations determining the piece-wise constant D-values are:

$$\rho_{wcap} - \rho_{w1} = \frac{\sqrt{\pi} A_N}{2\sqrt{D_1}} \operatorname{erf}\left(\frac{\eta_{N,1}}{\sqrt{D_1}}\right) \tag{150}$$

$$\begin{aligned} \rho_{w1} - \rho_{w2} &= \frac{A_N\sqrt{\pi}}{2\sqrt{D_2}} \exp\left(-\left(\frac{1}{D_1} - \frac{1}{D_2}\right)\eta_{N,1}^2\right) \cdot \\ &\quad \left(\operatorname{erf}\left(\frac{\eta_{N,2}}{\sqrt{D_2}}\right) - \operatorname{erf}\left(\frac{\eta_{N,1}}{\sqrt{D_2}}\right)\right) \end{aligned} \tag{151}$$

$$\vdots$$

$$\begin{aligned} \rho_{wN-2} - \rho_{wN-1} &= \frac{A_N\sqrt{\pi}}{2\sqrt{D_{N-1}}} \cdot \\ &\quad \exp\left(-\left(\frac{1}{D_1} - \frac{1}{D_2}\right)\eta_{N,1}^2 - \ldots \left(\frac{1}{D_1} - \frac{1}{D_2}\right)\eta_{N,N-2}^2\right) \cdot \\ &\quad \left(\operatorname{erf}\left(\frac{\eta_{N,N-1}}{\sqrt{D_{N-1}}}\right) - \operatorname{erf}\left(\frac{\eta_{N,N-2}}{\sqrt{D_{N-1}}}\right)\right) \end{aligned} \tag{152}$$

$$\begin{aligned} \rho_{wN-1} - \rho_{wN} &= \frac{A_N\sqrt{\pi}}{2\sqrt{D_N}} \cdot \\ &\quad \exp\left(-\left(\frac{1}{D_1} - \frac{1}{D_2}\right)\eta_{N,1}^2 - \ldots \left(\frac{1}{D_{N-1}} - \frac{1}{D_N}\right)\eta_{N,N-1}^2\right) \cdot \\ &\quad \left(1 - \operatorname{erf}\left(\frac{\eta_{N,N-1}}{\sqrt{D_N}}\right)\right) \end{aligned} \tag{153}$$

where for $N = 1$ one has $\rho_{wN-1} = \rho_{w0} = \rho_{wcap}$. A method for facilitating the calculation of the D_n from the above equations is described in [20].

The above described method to calculate the function D_w, using semi-infinite one-dimensional conditions for materials having a square root dependent mass gain during one-dimensional, semi-infinite, capillary suction, can also be described with the Kirchhoff potential ψ, e.g. see [18].

In report II:1 an alternative way of evaluating the capillary suction process is described. This approach is based on using both the momentum balance equation and mass balance equation for the capillary water, which is treated as a viscous fluid interacting with the pore walls. In this method the involved constants cannot be explicitly calculated as described in this section. The constants rather must be fitted to the measured global response in a more indirect manner.

3.4.3 Non-isothermal moisture transport with hysteresis and transient sorption

Building materials are in most cases subjected to environments where both temperatures and relative humidities vary. A model describing the moisture response for such environmental changes becomes much more involved when compared to isothermal conditions.

Some of the problems that must be dealt with in a non-isothermal case will be illustrated with a somewhat general description of the system. It should be observed that no direct simple experimental methods can be used to evaluate the material functions included in the model. The model rather has to be fitted to the experimental result by making a parameter study.

The temperature changes not only the flow properties of vapor and liquid water in the pore system of the material, but also the equilibrium condition between the vapor mass density concentration and the mass density concentration of liquid water, i.e. the absorption and desorption isotherms are changed. Experiments on vapor diffusion in bulk air show that the dependence of the diffusion coefficient for vapor on temperature is weak. Therefore, the great difference in responses in materials at different temperatures can be expected to be mainly due to the changes in the sorption and desorption behavior. Due to important effects on the sorption caused by temperature, it is difficult to incorporate non-thermal effects in the simple model as, for example, described by equations (100) and (101), which only involve one material function describing the flow characteristics of moisture in material. Furthermore, a simpler model assumes that the flow characteristics can be described with any state variable as indicated in equation (103). This assumption means that a given relation between the vapor mass density concentration (or the relative humidity) and the mass density concentration of liquid water in material must always be located at the sorption isotherm, e.g. see equation (104). In order to facilitate the introduction of non-isothermal

effects on moisture transport, this type of description will be abandoned in favor of a method where the sorption effects are decoupled from the global diffusion behavior. This method will also make the introduction of the hysteresis effect on sorption more direct and understandable. However, one of the drawbacks of the method to be presented is that two mass balance equations have to be considered, one for the vapor phase and one for the liquid phase. The reason for using these two equations is that the mass exchange between the phases, i.e. the sorption, will be described in a direct manner.

The mass balance for the liquid water in material is the postulate

$$\frac{\partial \rho_l}{\partial t} = -\frac{\partial}{\partial x}\left(\rho_l x_l^{'}\right) + \hat{r}_l \tag{154}$$

where ρ_l is the mass density concentration of liquid water in material, $x_l^{'}$ is the velocity of water and $\hat{r}_l$ is the gain of water from the vapor phase neighboring the water in the pores.

The mass balance postulate for the vapor in the pore system of material is

$$\frac{\partial \rho_v}{\partial t} = -\frac{\partial}{\partial x}\left(\rho_v x_v^{'}\right) + \hat{r}_v \tag{155}$$

where ρ_v is the mass density concentration of water vapor in the material, $x_l^{'}$ is the velocity of vapor and $\hat{r}_v$ is the gain of vapor from the liquid water in pores.

No net production of mass take place in the system, which means that the condition

$$\hat{r}_l = -\hat{r}_v \tag{156}$$

most hold. That is, effects caused by, for example, hydration are ignored.

The last mass balance principal considered in this model is a simple version of conservation of energy, i.e.

$$\frac{\partial \varepsilon}{\partial t} = -\frac{\partial h}{\partial x} \tag{157}$$

where ε is the internal energy for the whole system and h is the heat flux.

The constitutive assumption for the mass flow $\rho_l x_l^{'}$ of liquid water is

$$\rho_l x_l^{'} = -D_l\left(\rho_l\right)\frac{\partial \rho_l}{\partial x} - S_l\frac{\partial \theta}{\partial x} \tag{158}$$

where D_l is the diffusion parameter which is assumed to be dependent on the water mass concentration in the pore system and S_l is a material constant related to the gradient of temperature. The same type of assumption is used for the mass flow of the vapor in a pore system, i.e.

$$\rho_v x_v^{'} = -D_v(\rho_l)\frac{\partial \rho_v}{\partial x} - S_v\frac{\partial \theta}{\partial x} \tag{159}$$

where the diffusion parameter for vapor D_v is assumed dependent on the value of ρ_l. The heat flux in the system is assumed to be described by Fouriers law, i.e.

$$h = -\lambda(\rho_l)\frac{\partial \theta}{\partial x} \tag{160}$$

where λ is the thermal conductivity for the material. The parameter λ is assumed to be dependent on the mass density concentration of water in material porosity. The internal energy is assumed to be related to the temperature, as

$$\varepsilon = C(\rho_l)\,\theta \tag{161}$$

where C is the heat capacitance assumed to be dependent on the value of ρ_l.

The mass exchange rate between the vapor and liquid water is assumed to be given by the function ρ_v^{eq} and the constants R and n, as

$$\hat{r}_v = R(\rho_v - \rho_v^{eq})^n \tag{162}$$

where the function ρ_v^{eq} is the equilibrium condition for the vapor in contact with the water phase. The material coefficients R and n are analyzed, for cement mortar, in paper 8.

The property ρ_v^{eq} is a function not only of the mass concentration of water ρ_l and temperature θ but also of the drying and wetting history, i.e.

$$\rho_v^{eq} = \rho_v^{eq}(\rho_l, \theta, \text{'drying and wetting history'}) \tag{163}$$

This means that the adsorption and desorption isotherms must be measured for several temperatures, i.e. sorption measured from zero relative humidity up to 100% and then back to zero. Furthermore, so-called scanning curves must be measured, which involve equilibrium conditions between mass concentration of water and vapor in material during different conditions in terms of wetting-drying histories, different from the one mentioned above, i.e. the 0-100-0% relative humidity cycle.

The kinetics of sorption, according to equation (162), are assumed to be related to the 'distance' between the actual value of the mass density concentration of vapor ρ_v in the material and the equilibrium value ρ_v^{eq} given from the sorption isotherm at the current temperature θ and for a given history in terms of drying and wetting.

The governing equation for the mass density concentration of liquid water $\rho_l(x,t)$ is obtained by combining the mass balance equations (154) and (156), and the two constitutive equations (158) and (162), yielding

$$\frac{\partial \rho_l}{\partial t} = \frac{\partial}{\partial x}\left(D_l(\rho_l)\frac{\partial \rho_l}{\partial x} + S_l(\rho_l)\frac{\partial \theta}{\partial x}\right) - R(\rho_v - \rho_v^{eq})^n \tag{164}$$

where ρ_v^{eq} is given by a function of the type illustrated in (163).

The governing equation for $\rho_v(x,t)$ is obtained by combining the mass balance equation (155) and the two constitutive equations (159) and (162), which results in the expression

$$\frac{\partial \rho_v}{\partial t} = \frac{\partial}{\partial x}\left(D_v(\rho_l)\frac{\partial \rho_v}{\partial x} + S_v(\rho_l)\frac{\partial \theta}{\partial x}\right) + R(\rho_v - \rho_v^{eq})^n \tag{165}$$

The equation for determination of the temperature field $\theta(x,t)$ is obtained by combining (157) and (160), yielding

$$\frac{\partial (C(\rho_l)T)}{\partial t} = -\frac{\partial}{\partial x}\left(\lambda(\rho_l)\frac{\partial \theta}{\partial x}\right) \tag{166}$$

In paper 8 the concept of dividing the moisture flow into two phases, as described in this section, is used. The results are compared with measurements and modeling given in [21]. The method has also been described in [22].

3.4.4 Methods of measurements of moisture profiles

The information obtained from the equilibrium conditions between moisture content and relative humidity is not sufficient for obtaining moisture transport models. The flow properties must also be considered. One way is to fit models to measured moisture profiles for given exposure conditions. Here different experimental techniques for measuring moisture profiles will be discussed, e.g. see [20].

Slice-dry-weight method: The moisture content of material exposed to unidirectional liquid water or water vapor is measured by removing parts or slices (cut perpendicular to the flow) that are weighed, dried and weighed again. The removed material is collected from different distances from the exposed surface. The drying process can be performed in an oven at temperatures just above 100°C or, in the case of heat sensitive materials, an exciccator with a drying agent such as silica gel or sulfuric acid.

Electrical methods: The content of moisture in material can be measured by variations of electric conductivity (resistance) or by the variation of the electrical capacitance, e.g. see [23]. Both methods are non-destructive tests. The conductivity is measured by two electrodes in direct contact with the material. The method must be calibrated against the specific material tested at several different moisture contents. One problem associated with measurements on concrete is that the presence of ions in a pore solution will significantly affect the test results.

Gamma-ray attenuation: The gamma-ray attenuation method for measuring moisture contents in materials is a non-destructive test. The method is based on a gamma ray source and a detector which are placed on the sides of the specimen, e.g. see [24]. The source can consist of Am^{241}, Cs^{137} or Co^{60}. The detector is usually a scintillation crystal, e.g. a NaI crystal. The gamma ray (photons) interact with the orbital electrons in the material and are absorbed or scattered. The intensity of a narrow beam of gamma rays passing through a material can be expressed as $I = I_o e^{-\mu\rho x}$, where I [counts/s] is the gamma ray intensity after passing through the material, I_o [counts/s] is the reference intensity without absorbing material, μ [m^2/kg] is the mass adsorption coefficient of the tested material, ρ is the tested material density and x is the thickness of the material sample or, equally, the distance between source and detector. The equipment must be calibrated against the specific material tested.

Neutron radiography: In this method neutrons are used instead of gamma rays. The benefit is that the attenuation of a neutron beam, caused by scattering and adsorption of the neutrons, mainly interacts with the hydrogen nuclei, hence the attenuation can be directly related to the total water content in the material. The intensity of a neutron beam passing through a

sample is described by an expression similar to the one of the intensity of gamma rays, i.e. $I = I_o e^{-x(\mu_{mat}+\mu_w \varepsilon)}$, where μ_{mat} [m^{-1}] and μ_w [m^{-1}] are the macroscopic attenuation coefficient of the specific material and of water, respectively, and ε [m^3/m^3] is the water content volume by volume material. The neutron beam can be produced by a combination of boron and cadmium, and the neutrons can be detected by a ^{3}He proportional detector. Results from measurements with neutron radiography on different materials and experimental arrangements are shown in, for example, [25].

Nuclear magnetic response (NMR): In a NMR experiment an exterior permanent magnetic field is applied. When an electromagnetic field is applied, perdenticular to the constant magnetic field, energy is adsorbed. The energy adsorbed is proportional to the number of hydrogen nuclei in the measured volume of material, hence the water content in the material can be evaluated. Two benefits of the NMR method as compared to the gamma-ray attenuation and neutron radiography methods are that the NMR is directly related to the amount of hydrogen nuclei and that no radioactivity is involved during the experiment. Examples of results from measurements with NMR are shown in [26].

Computer tomography: The intensity loss of a narrow beam of X rays passing through the specimen is used in this method. The adsorption is a measure of the density of the specific material tested. The adsorption of X rays in dry concrete is about 145-150% greater than the adsorption in water, e.g. see [27].

Microwave beam: A specimen is placed between a transmitter and a receiver. The attenuation of the microwave beam caused by the oscillation of water molecules is measured. The magnitude of the attenuation corresponds to the water content in the material. The method must be calibrated against the material in question. The measuring technique is, for example, in detail described in [28].

Thermal conductivity: By locally producing a temperature gradient in material using a heat source, and by measuring the temperature vs. time curve at a certain distance from the heat source, the thermal conductivity

can be estimated, e.g. see [29]. If the relation between the moisture content and conductivity is known, the moisture content can be calculated from the experimental results. The induced temperature gradient may, however, influence the moisture flow, which is a source of error.

Thermal imaging: This method is based on the fact that the temperature of a material surface decreases when water at or near the surface evaporates, e.g. see [30]. A sample is split into two halves perpendicular to the exposed surface. The temperatures of the split surfaces are measured with an infrared camera. Methods to calculate the moisture content from the measured temperatures have been proposed. Another method is to calibrate the measured temperatures of the split surfaces against the temperature of split surfaces of well-conditioned specimens.

3.5 Moisture fixation

3.5.1 Methods of measurements of the equilibrium moisture content in materials

The moisture condition in concrete is, as discussed earlier, one of the most important factors affecting the diffusion characteristics of ions dissolved in a pore solution. Measurements of relevant properties concerning moisture levels and the moisture flow lead to models which can be incorporated into other models dealing with ion diffusion in a pore solution. This subject is treated in section 3.3.2.

Measurements of the moisture conditions in materials normally consist of two parts, i.e. the measurements of the equilibrium conditions between different vapor pressures and water contents in the material, and the measurements of the mass flow of moisture at different water contents in the material. Different techniques to measure the equilibrium moisture content for different relative humidities will be discussed below.

Climate box method, direct method: Samples are placed above saturated salt solutions in tightened boxes. Different salt solutions give different saturation pressures, i.e. relative humidities, at given temperatures. The samples can initially be either saturated or dried depending on whether the desorption or absorption isotherm is to be measured. The experiment is ended when the samples are stabilized in weight.

Results from sorption isotherms measured with the climate box method, on different building materials, can be found in paper 4.

Sorption balance: The sorption balance instrument consists of a very sensitive, symmetrically arranged micro-balance placed in a temperature controlled chamber. The relative humidity near the sample is obtained by mixing dry and saturated air using flow regulators. The balance continuously measures the weight, hence the kinetics of sorption can be measured as well as the equilibrium isotherm. Sample weights in the range of 25-200 mg can be used. An equilibrium adsorption isotherm can be obtained by letting the system increase the relative humidity surrounding the sample, e.g. in a certain number of steps from dry to 95% relative humidity. The criterion for proceeding to a higher relative humidity is, typically, a prescribed value of the rate of mass change of sample. The desorption isotherm is obtained

in the same manner starting with a saturated sample which is dried in certain relative humidity steps down to zero relative humidity. The moisture transport to and from the sample is facilitated by the flow of gas passing the relatively small sample; the surface resistance for moisture leaving or entering the sample is, therefore, decreased.

The sorption balance technique is used to investigate different materials in reports III:1-2 and papers 4 and 6-7.

Pressure plate method: This is an indirect method for measuring equilibrium moisture isotherms at high moisture contents. The method is indirect in the sense that the externally supplied pressure on the sample must be converted to a corresponding relative humidity using the so-called Kelvin relation. One of the main benefits of the method is that points in the desorption isotherm can be measured very near 100% relative humidity. Furthermore, the applied pressures corresponding to relative humidities in the range of approximately 92 to values close to 100% can be adjusted very accurately. In papers 4 and 6 the method is used to measure desorption at high moisture contents on different building materials.

Calorimetric method: Like the pressure plate method, the calorimetric method is indirect in the sense that the relative humidity in a sample chamber must be calculated from the flow characteristics of water vapor in the instrument, see reports III:1-2 and papers 4 and 5. The instrument consists of two chambers connected with a thin tube. One of the chambers, referred to as the vaporization chamber, contains liquid water and the other contains a dry sample. The liquid water in the vaporization chamber is transported through the thin tube into the sample chamber. The flow of vapor leaving the liquid surface in the vaporization chamber is continuously measured by registering the thermal power near the chamber by using thermocouples. Quasi-static assumptions are used to predict the development of the relative humidity in the sample chamber (which initially is zero) during the run. Furthermore, it is assumed that the flow leaving the vaporization chamber is the same as the flow entering the sample chamber, i.e. no transient diffusion in the tube can be accepted. Moreover, the vapor reaching the sample is assumed to be immediately adsorbed onto the sample material surfaces. If thermocouples are also placed at sample chamber, the heat of adsorption for the studied material can be evaluated. The method is described in [31].

3.5.2 Measurements of specific surface area and pore size distribution

The specific surface area of concrete very much determines the reactivity between ions dissolved in pore solution and the solid hydration products. The pore size distribution is an important property determining diffusion velocities of gases in air filled space or ions dissolved in pore solution.

The specific surface area and pore size distribution cannot be measured in any direct manner. The determination of the specific surface area for a material is based on sorption measurements together with assumptions introduced in the BET theory, e.g. see [32] and [33]. Therefore it is very important to judge the results from such investigations from the necessary assumptions leading to the BET equation. These assumptions are analyzed in this section. Furthermore, the assumptions leading to the so-called Kelvin and Laplace relations are discussed. These relations serve as a basis for evaluating the pore size distribution from desorption measurements.

In the BET theory it is assumed that the vapor pressure p and the surface area s_{i-1} occupied by $i-1$ discrete molecule layers are related to the surface area s_i, the 'activation' heat E_i involved in placing molecules in the i:th adsorbed layer and the temperature θ, as

$$a_i p s_{i-1} = b_i s_i e^{-E_i/(R\theta)}; \qquad i = 1, 2, ..., \infty \tag{167}$$

where a_i and b_i are material constants and R is the gas constant. The relation (167) is established from the condition that the condensation rate of molecules onto the $i-1$ layer ($i = 0$ is the bare surface) is equal to the evaporation rate from the i:th adsorbed layer. The condensation rate onto layer $i-1$ having the surface area s_{i-1} is assumed to be given by the pressure p above adsorbed layers as $a_i p s_{i-1}$, where a_i is a constant, and the condensation rate from layer i is assumed to be proportional to the surface area s_i and the Arrhenius factor $e^{-E_i/(R\theta)}$ through the material constant b_i as $b_i s_i e^{-E_i/(R\theta)}$.

By summing the surface areas occupied by the different discrete clusters, having different numbers of layers, one obtains the total surface area A occupied by the adsorbate, as $A = \sum_{i=0}^{\infty} s_i$. Further, the total volume of the adsorbed gas is $v = v_o \sum_{i=0}^{\infty} i s_i$, where v_o represents the volume of adsorbate on the adsorbent surface per unit area of the material when covered by a complete unimolecular layer (water molecules in the first layer is covered by molecules in additional layers).

The ratio $v/(Av_o)$ is formed as

$$\frac{v}{Av_o} = \frac{v}{v_m} = \frac{\sum_{i=0}^{\infty} is_i}{\sum_{i=0}^{\infty} s_i} \tag{168}$$

where $v_m = Av_o$ represents the volume of adsorbed gas corresponding to a complete monolayer.

The standard BET equation to be derived includes the assumption that only the molecules included in first formed layer have a condensation heat different from normal condensation. Assuming that $E_2 = E_3 = ... E_i = E_L$, where E_L is the heat of liquefaction, i.e. the condensation heat involved in creating discrete layers is the same for all layers greater than one, assuming, further, that $b_2/a_2 = b_3/a_3 = ... b_i/a_i = g$, where g is a constant, the following can be established

$$s_1 = ys_o \tag{169}$$

where (167) is used and where $y = (a_1/b_1)\, pe^{E_1/(R\theta)}$. Further, one obtain

$$s_2 = xs_1 \tag{170}$$

where $x = (p/g)\, e^{E_L/(R\theta)}$. Note also that $s_i = xs_{i-1}$ holds for all $i > 1$, due to the above described simplifications. By combining such equations one can for example establish that $s_3 = xs_2 = x^2 s_1$. More generally, for $i > 1$, one obtains the relations

$$s_i = xs_{i-1} = x^{i-1}s_1 = yx^{i-1}s_o = cx^i s_o \tag{171}$$

where $c = y/x = \frac{a_1 g}{b_1} e^{(E_1 - E_L)/(R\theta)}$. That is, s_1, s_2, s_3, ... s_i can be expressed in terms of s_o by the constant c and different powers of x.

By using $s_i = cx^i s_o$ given from (171), the equation (168) can be rewritten as

$$\frac{v}{v_m} = \frac{cs_o \sum_{i=1}^{\infty} ix^i}{s_o\left(1 + c\sum_{i=1}^{\infty} x_i\right)} \tag{172}$$

To be able to write the term v/v_m as a function of x, one can, for example, assume that an infinite number of layers can be formed. In such a case

the sums included in equation (172) converge, as $\sum_{i=1}^{\infty} x_i = x/(1-x)$ and $\sum_{i=1}^{\infty} ix^i = x/(1-x)^2$. That is, when assuming that an infinite number of layers can be formed, the term v/v_m is a function of x given as

$$\frac{v}{v_m} = \frac{cx}{(1-x)(1-x+cx)} \tag{173}$$

That is, the BET equation (173) expresses the total volume of adsorbate v as a function x, and the material parameters c and v_m are used to fit the measured sorption isotherm. By noting that when $v \longrightarrow \infty$ in the expression (173), one must have $x \longrightarrow 1$. It is, further, assumed that when $v \longrightarrow \infty$ the pressure above adsorbate must be saturated, i.e. $p = p_o$. From the definition $x = (p/g)\, e^{E_L/(R\theta)}$ it is concluded that x can be interpreted as the relative vapor pressure $x = p/p_o$.

For the case when assuming the two first layers to have a condensation heat different from normal condensation heat, one obtains the BET equation

$$\frac{v}{v_m} = \frac{cx\,(1+(b-1)\,(2x-x^2))}{(1-x)\,(1+(c-1)\,x+(b-1)\,x^2c)} \tag{174}$$

where the property c again is defined as $c = (a_1 g/b_1)\, e^{(E_1-E_L)/(R\theta)}$, and where b is defined as $c = (a_2 g/b_2)\, e^{(E_2-E_L)/(R\theta)}$. In reports III:1-2 the 'one layer' and 'two layer' BET equations, i.e. (173) and (174), are used to calculate the specific surface area on porous glass. In these two reports the material constant ratios $(a_1 g/b_1)$ and $(a_2 g/b_2)$ are calculated by indirect measurements on the condensation heats E_1 and E_2 obtained from the calorimetric technique described in section 3.5.1. The obtained values of $(a_1 g/b_1)$ and $(a_2 g/b_2)$ differed significantly from the often proposed values of unity.

Consider next the evaluation of the pore size distribution. The pore size distribution can be estimated by using the measured desorption isotherm together with the Kelvin formula and the Laplace equation. During equilibrium defined by isothermal conditions and when no net mass exchange between vapor and adsorbed or capillary condensed water takes place, the relation between the chemical potential in the vapor and the adsorbed or capillary condensed water is given as

$$\frac{\partial \mu_v}{\partial \rho_v} = -\frac{\partial \mu_a}{\partial \rho_a} \tag{175}$$

where the chemical potential for the vapor μ_v and for the adsorbate μ_a are allowed to be functions of the temperature θ and mass density of vapor ρ_v and

of adsorbate ρ_a only, i.e. $\mu_v = \mu_v(\theta, \rho_v)$ and $\mu_a = \mu_a(\theta, \rho_a)$. This assumption is referred to as the simple fluid assumption since μ_v is not allowed to depend on ρ_a and vice versa. The relation (175) is obtained by considering the second axiom of thermodynamics together with the physical balance laws for the special constitutive relations $\mu_v = \mu_v(\theta, \rho_v)$ and $\mu_a = \mu_a(\theta, \rho_a)$. Another relation which can be established by the same method, for this case, is a relation between the chemical potential of the adsorbate μ_a and the pressure in adsorbate p_a during isothermal conditions, given as

$$\rho_a \frac{\partial \mu_a}{\partial \rho_a} = \frac{\partial p_a}{\partial \rho_a} \tag{176}$$

Assume, further, that the explicit constitutive relation for the chemical potential for the vapor is given as

$$\mu_v(\theta, \rho_v) = C_v\theta(1 - \ln\theta) + \frac{R}{M_v}\theta \ln \rho_v \tag{177}$$

By combining (175), (176) and (177) one obtains

$$\frac{\partial p_a}{\partial \rho_a} = -\frac{\rho_a R\theta}{M_v \rho_v} \tag{178}$$

which expresses the relation between the pressure in the vapor and the adsorbate. The integrated version of (178), with opposite sign (i.e. $p_a = -p_{cap}$), can be interpreted as the so-called capillary pressure, i.e.

$$p_{cap} = \int_{\rho_v}^{\rho_{vs}} \frac{\rho_a R\theta}{M_v \rho_v} = -\frac{\rho_a R\theta}{M_v} \ln\left(\frac{\rho_v}{\rho_{vs}}\right) = -\frac{\rho_a R\theta}{M_v} \ln(x) \tag{179}$$

where integration from actual vapor mass density concentration ρ_v to saturated concentration ρ_{vs} is used. It is also assumed that ρ_a remains constant, that is, for water $\rho_a = 1000$ kg/m^3.

The pressure p_{cap} can be assumed to be related to the mean curvature r_{cap} of the capillary condensed liquid through the material constant γ_a, which represents the surface tension of the adsorbate (or equally the surface energy). This relation is the Laplace equation, i.e.

$$p_{cap} = \gamma_a \left(\frac{1}{r^1_{cap}} + \frac{1}{r^2_{cap}}\right) = \frac{\gamma_a}{2r_{cap}} \tag{180}$$

where r^1_{cap} and r^2_{cap} are the radii of the curvature of the meniscus in two orthogonal directions. The property r_{cap} does not need to be equivalent to the pore radii in which the liquid is present if the so-called wetting angle α is different from zero. When allowing for different wetting angles between liquid and material, the relation between the radii r_{cap} and the pore radii r_{pore} becomes

$$r_{cap} = \frac{r_{pore}}{\cos(\alpha)} \tag{181}$$

In this relation the effect of adsorbed layers on the evaluation of the pore radii r_{pore} is ignored.

From the relations (179), (180) and (181) the pore distribution can be estimated, i.e.

$$r_{pore} = -\frac{M_v 2\gamma_a \cos(\alpha)}{\rho_a R\theta \ln(x)} \tag{182}$$

It should be noted that when the relative humidity is low the adsorbed liquid does not necessarily wet the material in narrow pores. Therefore the use of (182) should be restricted to medium and high relative humidities. It should also be noted that different pore size distributions, calculated from expression (182), will be obtained depending on whether the measured desorption or adsorption data are used.

4 Reports

4.1 Short introductions to reports, Part I: Chloride ingress

4.1.1 Report I:1, A study of diffusion and chemical reactions of ions in pore solution in concrete exposed to chlorides

This report is an extension of the paper *Diffusion of a mixture of cations and anions dissolved in water* (paper 1), in the sense that it allows for diffusion of a mixture of different ion types in the pore solution of concrete. Here chemical reactions are also included. The reactions considered are binding and dissolution of chlorides and dissolution of hydroxide from solid calcium-hydroxide in the hydration products. A model similar to the one described in section 3.3.2 and a method of solving the equations in the model are developed. Experiments are performed on chloride penetration on three different concrete qualities. The experimental method involves measurements of chloride profiles as described in section 3.3.3 (ion selective electrode). The material constants in the model are chosen so as to provide the best match to the experimentally obtained data on chloride profiles. The number of unknown material constants is kept to a minimum by assuming that the diffusion constants and ionic mobilities in bulk water can be used together with a tortuosity factor which is identical for all different types of ions. The problem is, therefore, very much directed to the determination of the material constants describing the chemical reactions.

The numerical solution procedure is described in the report. The coupled equations are arranged in such a way that the system of equations can be solved in one step only at every time level. This approach avoids many of the problems involved in the staggering solution procedure.

The model is able to simulate the experimentally observed phenomenon that a maximum concentration in the chloride profile is at about 3-6 mm from the exposed surface. This result cannot be obtained if dielectrical effects among positive and negative ions in pore solution are not included. If the model is to be relevant it is observed that as many as possible of the common ions present in the pore solution of the cement-based material should be considered, as they will affect the diffusion of chlorides. Seven constituents are considered in the model. The calculated profiles of these constituents are presented.

4.1.2 Report I:2, The effect of different cements and pozzolans on chloride ingress into concrete

In this report the model established in *A study of diffusion and chemical reactions of ions in pore solution in concrete exposed to chlorides* (report I:1) is used to study the effect of different cements and pozzolans on chloride ingress. The model is described again, but in a more direct manner as compared with report I:1. The numerical treatment is, however, excluded. From the experiments it was found that OPC (ordinary Portland cement) concrete with 5% silica fume resisted chloride ingress better than other binder types studied. It was also concluded that silica fume worked better when mixed with OPC than when mixed with SRPC (sulfate resistent Portland cement). A mixture of fly ash and silica fume used together with SRPC was also tested. 20% fly ash and 5% silica replacing SRPC was shown to improve the resistance to chloride ingress as compared to when using pure SRPC not replaced by any pozzolans.

From simulations it was concluded that the tortuosity factor and binding capacities of chlorides were correlated to the porosity and cement content, when comparing the same cement type. However, when comparing different types of concrete mixes including different cements and pozzolans, such correlations could not be found. It was therefore concluded that not only the porosity developed by the cement and pozzolan used is of importance, but also the shape of the pore system.

4.1.3 Report I:3, The effect of curing conditions on chloride ingress in concrete

Three different curing conditions, and their effects on chloride penetration, are examined experimentally. One of the curing methods includes a period of drying and re-wetting in tap water before exposure to chloride. The drying was shown to be a positive factor making the penetration of chloride slower. According to the tortuosity factors obtained by matching the experimentally obtained chloride profiles with simulations, drying makes the pore system denser in the sense that ions penetrate more slowly. It was also observed that samples directly exposed to chlorides, and samples stored for one week in tap water before exposure, had about the same penetration rates of chloride.

One result obtained from simulation is that one possible explanation of the commonly observed phenomenon that the maximum chloride concen-

tration occurs at a depth of a few millimeters from the exposed surface, a phenomenon most dominant for samples dried before exposure, is due to a combined effect of dielectrics, i.e. the effect on the diffusion velocities of different types of ions due to their valence charges, and dissolution of hydroxide ions from solids. That is, according to the model a sample pre-dried and re-saturated before exposure dissolves hydroxide more easily than 'virgin' samples not dried before exposure.

4.2 Short introductions to reports, Part II: Moisture transport

4.2.1 Report II:1, Modeling of a viscous fluid percolating a porous material due to capillary forces

The concentration characteristics of different types of ions in a pore solution are very much affected by the moisture conditions. One important factor is that capillary suction of water containing ions makes the ions penetrate the material faster than compared with the case when ion transport occurs by diffusion only. The possibility of describing the combined ion transport by diffusion and convection, due to capillary suction, is therefore very important. In the report a new method of treating the capillary suction is developed without allowing for the effect of ions. The method is based on the fact that the water can be described as a viscous fluid, i.e. it can sustain shear stress while in motion. It is further assumed that the solid pore wall influences the fluid by assuming that a force is acting between the fluid and the solid. This force is assumed to be proportional to the difference of velocities of the fluid and the solid. The solid velocity is of course assumed to be zero. This method of describing capillary suction is essentially different from the one described in section 3.4.2. The conclusions drawn from this new model can therefore contribute to knowledge of the mechanisms behind capillary suction not available from evaluating the classical hypothesis.

The results from the simulations for a certain choice of material constants showed that the mass gain due to capillary suction was proportional to the square root of exposure time, which is a common experimentally observed case for many different types of porous materials. Problems of identifying proper boundary conditions for the fluid equation describing the velocity field of the capillary sucked water were, however, observed. It was suggested that a momentum pulse should be use instead of a prescribed pressure at the

boundary.

4.3 Short introductions to reports, Part III: Moisture fixation

4.3.1 Report III:1, Verification of the BET-theory by experimental investigations on the heat of adsorption

From the BET theory the specific surface area can be evaluated from the measured sorption isotherms. Furthermore, the heat required to place molecules in the first monolayer close to the surface and in higher layers can be predicted by the BET-theory. The calorimetric technique developed enables the measurement of the heat of (global) sorption as a function of the relative humidity. In order to compare the measured heat of sorption with the heats required to create different discrete adsorbed layers on a material surface, as proposed by the BET theory, the distribution of total adsorbate among different layers must be known. In the report it is shown that this distribution can be derived from the basic assumptions included in the BET equation.

Two materials were tested, porous glass and microcrystalline cellulose. It was shown that the development of molecule layers on porous glass as predicted by the BET theory and the measured heat of adsorption agreed well. The predicted heat of adsorption of the first layer using the BET theory was, however, found to be a factor 2.5 less than the measured value. It was, therefore, suggested that a certain ratio related to the rate of adsorption of a given layer to that of bulk water, which in the BET theory usually is explicitly assumed to be equal to unity, instead should be chosen in a way giving the best fit to measured data.

The microcrystalline cellulose did not follow the development of adsorption heat as a function of relative humidity in the way predicted by the BET theory. This result was observed even though a perfect match of the BET-equation to the measured adsorption isotherm was obtained. That is, the development of adsorption and the heat of adsorption as a function of relative humidity are not coupled, as suggested by the BET theory. This is probably due to chemically related action or/and capillary condensation, which effects are not included in the BET model, and being important even at low and medium relative humidities when testing microcrystalline cellulose.

It is concluded that the relevance of the BET equation can be tested by measuring both the adsorption isotherm and the heat of adsorption as a

function of the relative humidity. This becomes very important for material such as concrete for which the adsorption isotherm most probably is a result also of factors other than those on which the BET theory is founded. The evaluation of the specific surface area based on the BET equation could, therefore, be questioned when studying such materials.

4.3.2 Report III:2, Adsorption on porous Vycor glass at different temperatures at low and medium relative humidities

In this report, material functions describing the effect of varying temperatures on the adsorption isotherm are investigated. It is shown that these material functions are very sensitive to the temperature level. It was possible to reproduce the measured isotherms at different temperatures with only three material functions being dependent on temperature. According to the BET equation one of these material functions is directly proportional to the specific surface area of the material in question. This function was, however, forced to be changed significantly with temperature in order to match the experimentally obtained isotherms measured at different temperatures. The change of specific surface area with temperature was shown to be smaller when assuming a BET equation valid for a case where adsorbed molecules present in the two first layers have an adsorption heat different from the normal condensation heat of bulk water. The use of this kind of assumption was further strengthened by the fact that a better match between measured heat and predicted heat of condensation as a function of relative humidity was obtained for this case.

It was, furthermore, concluded that the predicted specific surface area becomes different depending on using the 'one layer' or 'two layer' BET equation, i.e. depending on whether one layer or two layers have an adsorption heat different from the normal condensation heat of bulk water.

5 Papers

5.1 Short introduction to papers

5.1.1 Paper 1, Diffusion of a mixture of cations and anions dissolved in water

This paper deals with diffusion of a mixture of positively and negatively charged ions. The problem is solved by assuming that not only the gradient of the concentration gives the diffusion flow but also the gradient of a electric potential. The electric potential is due to positive and negative ions being forced to diffuse in such a way that the net charge of the mixture is very close to zero. A numerical method is established capable of solving the coupled set of differential equations. The conclusions from the simulation of five different type of ions in a mixture are that the requirement of electron-neutrality affects the diffusion behavior of the individual ions very much, and that ions with a low diffusion coefficient will be diffused faster if mixed with ion types with comparably high diffusion coefficients. A simplified version of the model described in section 3.3.2 is used in this investigation, i.e. only diffusion in bulk water is considered, without any attention to chemical reactions.

5.1.2 Paper 2, Nonlinear transient phenomena in porous media with special regard to concrete and durability

Chloride penetration caused by 'pure' diffusion combined with convection is treated in this paper. A test example where chloride contaminated water is allowed to be capillary sucked into concrete is examined numerically. This case is compared to a case of pure diffusion. The velocity of the capillary sucked water at different spatial positions and at different time levels is calculated by using the moisture diffusion data given in [19]. Binding of chlorides is also included in the model. The results indicate that the capillary suction affects the penetration of chlorides to a very high degree. A simplified version of the model described in section 3.3.2 is used in which the dielectric effects are ignored.

5.1.3 Paper 3, Convection-diffusion problems with significant first-order reversible reactions

The solution of equations including convective terms cannot be accomplished by conventional methods. For example, when solving problems of combined diffusion and convection caused by capillary suction, it becomes important to establish special types of numerical techniques. In this paper a numerical weighting method called Petrov-Galerkin is tested, e.g. see [34] and [35]. The method is capable of solving equations including convective terms with an acceptable precision. The typical time scales for diffusion and binding of ions in porous materials are tested for a two-dimensional problem. The method is shown to be adequate for the applications of practical interest. That is, the numerical approach solves the equations correctly. The method is used to solve the equations presented in the paper 2, *Nonlinear transient phenomena in porous media with special regard to concrete and durability.*

5.1.4 Paper 4, A test of four different experimental methods to determine sorption isotherms

The properties of concrete and other porous materials are very much determined by their moisture conditions. One of the most important properties determining moisture condition is the sorption isotherm. The sorption isotherm is also of interest when establishing moisture diffusion models, and it can be used to evaluate the specific surface area and the pore size distribution of the material. Further, the surface area is one of the main properties related to chemical actions in concrete, such as binding of chloride and dissolution of hydroxide. The pore size distribution is of great importance with regard to diffusion of ions in a saturated pore system.

Different experimental methods for determining sorption isotherms are investigated in the paper. These methods are: *(i)* the climate box method, *(ii)* the sorption balance method, *(iii)* the pressure plate method and *(iv)* an indirect method referred to as the calorimetric approach. A short presentation of these methods can be found in section 3.5.1. A good agreement between the different methods was obtained for the tested sandstone and porous glass investigated.

5.1.5 Paper 5, Restrictions on the rate of adsorption when evaluating sorption isotherms from measurements using a microcalorimetric technique

In this paper a newly developed calorimetric technique for measuring sorption isotherms is investigated further. It turns out that if the kinetics of adsorption on the tested material are very slow, the method fails. A rate constant related to the sorption isotherm is defined. Simulations are performed in which different rate constants are tested. A range in which the rate constant gives acceptable reproduction of the sorption isotherm using the calorimeter is derived. The rate constant for different materials can be evaluated from measurements using the sorption balance. That is, the sorption balance can be used to check if the material can be successfully tested for sorption properties in the calorimeter.

From this paper it is also concluded that if only the heat of sorption as a function of relative humidity is of interest the rate effect, if any, can be compensated for if relevant properties are examined using parallel measurements in the sorption balance instrument.

5.1.6 Paper 6, Measurement of the moisture storage capacity using sorption balance and pressure extractors

In this paper measurements of the moisture storage capacity are presented for several porous building materials. Two complementary methods are investigated: the sorption balance and the pressure plate extractor. The sorption balance enables the user to measure sorption in the range of 0-95% relative humidity and the pressure plate extractor in the range of 92 to values very near 100% relative humidity. The measurements using the two different techniques in the interval in which the methods overlap, i.e. 92-95% relative humidity, show a satisfactory match.

5.1.7 Paper 7, Micro-structural changes caused by carbonation of cement mortar

The effect of carbonation on cement mortar on the specific surface area and pore size distribution are measured by sorption experiments. Ordinary Portland cement mortar samples were stored either in a chamber with an increased carbon dioxide content of maximum 1 vol. % or in a chamber free from carbon dioxide. After about 4 months the samples stored in the carbon

dioxide chamber proved to be fully carbonated. Powder from the carbonated and non-carbonated samples was then tested for water adsorption and desorption using a DVS-1000 sorption balance, see section 3.5.1. One of the benefits of this instrument, in this special application, is that the samples are not exposed to carbon dioxide during testing. Using the BET theory together with the measured adsorption isotherms it was shown that the non-carbonated sample had an 8% higher specific surface area as compared to the well-carbonated sample. The use of the measured desorption isotherms and the Kelvin equation showed that the well-carbonated mortar sample had about twice as much volume attributed to small pores as compared with the non-carbonated cement mortar.

5.1.8 Paper 8, Pre-study on diffusion and transient condensation of water vapor in cement mortar

A model dealing with diffusion of water vapor and transient condensation in cement mortar is established. One of the main aims was to construct a conceptual model which can easily be generalized to cases where non-isothermal conditions and hysteresis in the sorption behavior are included. The model was fitted against measurements on cement mortar, presented in [21], and a satisfactory match was obtained. The separate measurements performed on the water vapor sorption kinetics of cement mortar, using the sorption balance technique, did not, however, reflect the behavior found in [21]. The model used is a simplified version of the one presented in section 3.4.3.

References

[1] Mindess, S. and Young, J. F.(1981). *Concrete*, Prentice-Hall, Inc. Englewood Cliffs, New Jersey.

[2] Taylor, H.F.W. (1990). *Cement Chemistry*, Academic Press.

[3] Fagerlund, G. (1983). *Pozzolans in Concrete* (In Swedish), Cementa No 3 and 4, Stockholm.

[4] Sandberg, P. (1998). *Chloride Initiated Reinforcement Corrosion in Marine Concrete*, Lund Institute of Technology, Division of Building Materials, Lund.

[5] Ekström, T. (2000). *Leaching of Concrete, Experiments and Modelling*, Lund Institute of Technology, Division of Building Materials, Lund.

[6] Fagerlund, G. (1994). *Predicting the Service Life of Concrete Exposed to Frost Action Through a Modelling of the Water Absorption Process in the Air-pore System*, Lund Institute of Technology, Division of Building Materials, Report TVBM-7085, Lund

[7] Lindmark, S. (1998). *Mechanisms of Salt Frost Scaling of Portland Cement-bound Materials: Studies and Hypothesis*, Lund Institute of Technology, Division of Building Materials, Lund.

[8] Dahlblom, O. (1987). *Constitutive Modelling and Finite Element Analysis of Concrete Structures with Regard to Environmental Influences*, Lund Institute of Technology, Division of Structural Mechanics, Lund.

[9] Bowen, R.M. (1976). *Theory of Mixtures*, Part 1, in Continuum Physics, Edited by A. Cemal Erigen, Princeton University of Technology.

[10] Weast, R.C, Lide, D.R., Astle, M.J. and Beyer, W.H. (1989). *Handbook of Chemistry and Physics*, 70:th edition, CRC Press, Inc. Boca Raton, Florida.

[11] Collepardi, M. (1995). *Quick Method to Determine Free and Bound Chlorides in Concrete*, Proceeding of the RILEM International Workshop, Edited by Nilsson, L.O. and Ollivier, J.P, St-Rémy-lès-Chevreuse, France, pp. 10-16.

[12] Page, C.L., Short, N.R. and El-Tarras, A. (1981). *Diffusion of Chlorides in Hardened Cement Pastes*, Cement and Concrete Research, Vol. 11. pp. 751-757.

[13] Luping, T. (1996). *Chloride Transport in Concrete, Measurement and Prediction*, Chalmers University of Technology, Department of Building Materials, Göteborg.

[14] Janz, J and Johannesson, B.F. (1993). *A Study of Chloride Penetration into Concrete* (in Swedish), Lund Institute of Technology, Division of Building Materials, Lund.

[15] Nilsson, L.O., Massat, M. and Tang, L. (1994). *The Effect of Non-linear Chloride Binding on the Prediction of Chloride Penetration into Concrete Structures*, In Durability of Concrete: Proc. 3rd. Int. Conf., Edited by Malhotra, ACI SP 145, Detroit, pp. 469-486.

[16] Tuutti, K. (1982). *Corrosion of Steel in Concrete*, Swedish Cement and Concrete Institute (CBI), Royal Institute of Technology, Stockholm, Sweden.

[17] Alfarabi Sharif, Loughlin, K.F., Azad, A.K. and Navaz C.M. (1997). *Determination of the Effective Chloride Diffusion Coefficient in Concrete via a Gas Diffusion Technique.* ACI Materials Journal, Vol. 94, No. 3.

[18] Arvidsson, J. (1998). *Moisture Transport in Porous Media, Modelling Based on Kirchhoff Potentials.* Lund University of Technology, Department of Building Technology, Building Physics, Lund.

[19] Hedenblad, G. (1993). *Moisture Permeability of Mature Concrete, Cement Mortar and Cement Paste*, Lund Institute of Technology, Division of Building Materials, Lund.

[20] Janz, M. (1997). *Methods of Measuring the Moisture Diffusivity at High Moisture Levels*, Lund Institute of Technology, Division of Building Materials, Lund.

[21] Daïan, J.F. (1989). *Condensation and Isothermal Water Transfer in Cement Mortar: Part II - Transient Condensation of Water Vapor,* Transort in Porous Media Vol. 4. pp. 1-16, Kluwer Academic Publishers.

[22] Johannesson, B. (1998). *Modelling of Transport Processes Involved in Service Life Prediction of Concrete, Important Principles*, Lund Institute of Technology, Division of Building Materials, Lund.

[23] Krus, M. (1995). *Moisture Transport and Storage Coefficients of Porous Mineral Building Materials, Theoretical Principles and New Test Methods* (in German), Der Facultät Bauingenieur- und Vermessungswesen der Universität Stuttgart.

[24] Nielsen, A.F. (1972). *Gamma-Ray-Attenuation Used for Measuring the Moisture Content and Homogeneity of Porous Concrete*, Building Science, Vol. 7. pp. 257-263.

[25] Pel, L. (1995). *Moisture Transport in Porous Building Materials*, Eindhoven University of Technology.

[26] Kopinga, K. and Pel, L. (1994). *One-dimensional Scanning of Moisture in Porous Materials with NMR*, Rev. Sci. Instrum. 65 (12).

[27] Bjerkeli, L. (1990), *X-ray Tomography as a Method to Determine the Water Adsorption in Concrete* (in Norwegian), Report STF65 A90008, FCB, SINTEF, Trondheim.

[28] Wittig, G. and Lingott, H. (1992). *Investigation of the Moisture Transport in Building Materials by Microwave Beam* (in German), Bauphysik 14, Heft 2, pp. 44-49.

[29] Vos, B.H. (1995). *Non-steady-state Method for the Determination of Moisture Content in Structures, Humidity and Moisture*, Vol. 4, pp. 35-47, New York.

[30] Janz, M. and Johansson, P. (2000). *Evaluation of Thermal Imaging as a Method of Measuring Moisture Profiles over an Interface Between Cement-lime Mortar and Brick*, (manuscript), Lund Institute of Technology, Division of Building Materials, Lund.

[31] Wadsö, I. and Wadsö, L. (1996). *A New Method for Determination of Vapour Sorption Using a Twin Double Microcalorimeter.* Thermochimica Acta, Vol. 271, pp. 179-187.

[32] Brunauer S., Emmett P.H. and Teller E. (1938). *The Adsorption of Gases in Multimolecular Layers,* Journal of the American Chemical Society, 60.

[33] Brunauer, S. (1944). *The Adsorption of Gases and Vapours, Volume 1, Physical Adsorption.* Oxford University Press.

[34] Zienkiewicz, O.C. and Taylor, R.L. (1989). *The Finite Element Method, Fourth Edition, Vol. 2*, McGraw-Hill, London.

[35] Bathe, K.J. (1996). *The Finite Element Procedures*, Prentice Hall, Englewood Cliffs, New Jersey.